RESEARCH REPORT

VTT-R-02629-09

PRECASTEEL - WP 4: Optimization of seismic design of selected solutions

# Advanced analysis of the performance of steel frames

Authors: Ludovic Fülöp, Paul Beaucaire

Confidentiality: Confidential

Public after closing the project (July 2010).

| Report's title | |
|---|---|
| Advanced analysis and optimization of the structural performance of industrial steel frames | |
| Customer, contact person, address<br>Commission of the European Communities | Order reference<br>RFS-PR-06054 |
| Project name<br>Prefabricated steel structures for low-rise buildings in seismic areas | Project number/Short name<br>12597/PRECASTEEL |
| Author(s)<br>Ludovic Fülöp, Paul Beaucaire | Pages<br>43/(35+8) |
| Keywords<br>steel portal frames, design, FEM analysis, stability | Report identification code<br>VTT-R-02629-09 |

Summary

The document presents results of two types of advanced modeling for portal frames. In both cases, the frames were modeled as 3D shells in ABAQUS. Thus, it was possible to take into account buckling at the level of the member, (especially lateral and lateral-torsional buckling), but also local buckling at the level of the plates forming the flange and web of the elements. In all analysis cases the emphasis has been on the proper consideration of the support conditions (e.g. lateral support by purlins) of the frames.

Three types of portal frames are considered in the analysis. Members were made of (i) hot-rolled members, (ii) welded elements from plates and (iii) thin walled steel members. The first analysis method employed is based on a buckling and a strength analysis of the frame, and is in accordance with the design code prEN 1993-1-1. The second employed design method is based on non-linear (i.e. both geometrical and material) analysis under increasing loads, taking into account the initial imperfections of the frame.

In order to facilitate the creation and fast analysis of the frame models, the previously developed (VTT-R-00133-09), ABAQUS Plug-In based programs have been used.

The study shows that the SHELL based modeling is superior to beam based modeling especially when it comes to taking into account lateral-torsional buckling. Shell based modeling can also be economically feasible using tools similar to the developed ABAQUS Plug-In tools.

Public after closing the project (July 2010).

| Confidentiality | Confidential |
|---|---|

Espoo 15.4.2009

| Written by | Reviewed by | Accepted by |
|---|---|---|
| Fulop Ludovic<br>Senior Research Scientist | Talja Asko<br>Senior Research Scientist | Lehmus Eila<br>Technology Manager |

VTT's contact address
P.O. Box 1000, FI-02044 VTT, Finland

Distribution (customer and VTT)

| | |
|---|---|
| Customer (partners of RFCS project PRECASTEEL): | 1 pdf copy |
| VTT/Register Office: | 1 copy |

## Preface

This report contains material about possible design methods of portal frames, and examples of application for different configurations. The aim of the modeling was, to take into account as precisely as possible, the lateral-torsional buckling of frames; known to be one of the crucial designed challenges. For this purpose modeling based on SHELL finite elements has been adopted, fully considering the geometry of the framed, and the realistic support conditions.

The finite element models have been developed in the ABAQUS program, which is capable of handling both geometric and material nonlinearity. The development of such sophisticated FEM is rather time consuming and, in order to reduce the model generation time, plug-in based subroutines have been developed for ABAQUS. By using such subroutine, generating one frame model can take as little as a few seconds (The subroutines have been developed by Paul Beaucaire).

Results of two design methodologies are presented in this report: (i) the first one is based on a prEN 1993-1-1 procedure which uses buckling analysis together with elastic analysis; (ii) the second is based on nonlinear pushover taking into account the initial imperfections of the frames. Obviously the first methodology is less time consuming, as it supposes the carrying out of elastic analysis only (run time few seconds). The second procedure, based on for nonlinear method, can be much more time consuming (10-30 minutes).

Altogether, three configurations have been investigated based on use of: (i) hot-rolled profile, (ii) tapered welded and (iii) light-gauge steel (LGS) sections. The main conclusions of the report are that:

(1) Taking into account of the lateral-torsional buckling in classical, beam based, design is difficult. Several discrepancies have been found between frame configurations resulting from a beam based pre-design, and results of the more sophisticated SHELL based modeling.

(2) By using the adequate tools, SHELL based modeling can be brought to the level of being competitive, in terms of analysis time, with more simple analysis methods.

(3) It has been confirmed again, that frames are very sensitive to lateral-torsional buckling; and lateral support conditions of the frame play a crucial role in determining the performance. Support methods, believed to be adequate, have been shown to provide unsatisfactory performance.

(4) In all cases which were studied here, the determining design conditions for the frames were given by the vertical load combination. In no case the seismic load combination was controlling the designer of the frames.

Espoo, 15.4.2009

Authors

# Contents

## Abbreviations

LTB – lateral torsional buckling
PF's – portal frames
LB – local buckling
LGS – light-gauge steel
ULS – ultimate limit state
SLS – serviceability limit state
FEM – finite element method / finite element model

## Symbols

*Design properties of frames*

$\lambda_{OP}$ – non-dimensional slenderness
$\chi_{OP}$ – reduction factor corresponding to the non-dimensional slenderness
$\chi_{OP-1}$ – $\chi_{OP}$ calculated with prEN1993-1-1 Eq. 6.56 (see Figure 2)
$\chi_{OP-2}$ – $\chi_{OP}$ calculated with prEN1993-1-1 Eq. 6.57 (see Figure 2)
$\alpha_{cr,OP}$ – multiplier of loads to reach the smallest positive critical load
$\alpha_{ult,k}$ – multiplier of the loads to reach yielding
$\sigma_{max}$ – largest in-plane stress (component perpendicular to the cross-section)
$P_{DIST}$ – capacity of the frame at ULS for vertical loads; expressed as distributed load (self-weight of frame ignored)
$P_M$ – distributed load equivalent to the self-weight of the frame
$P_{ULS}$ – capacity of the frame at ULS for vertical loads; as distributed load (self-weigh considered, i.e. $=P_{DIST}-P_M$)
$P_{yield}$ – vertical distributed load causing yielding of the extreme fiber of the frame
$P_{des}$ – design load of the frame at ULS for vertical loads; represented as distributed load
$M_{fr}$ – mass of the frame
$M_{EQ}$ – mass on a frame in the earthquake combination (i.e. earthquake mass)
$P_{ULS-EQ}$ – distributed load on the frame in the earthquake load combination
$F_H$ – equivalent horizontal force for earthquake analysis with lateral force method

*Geometric dimension of frame/hall*

H – height of the portal frame
S – span of the frame
T – distance between frames

*Cross-section dimensions*

h – height of the cross-section
$h_c$ – height of the column cross-section
$h_h$ – height of the cross-section at haunch
$h_b$ – height of beam cross-section
b – width of cross-section (equal for column & beam in tapered frames)
$t_f$ – flange thickness
$t_w$ – web thickness

# 1 Introduction

Single story portal frames present design challenges especially due to buckling behavior, which is not easily evaluated and incorporated into the design calculations. The most significant mode of buckling for portal frames is lateral torsional buckling or LTB (Figure 1). LTB is difficult to account for, especially if modeling of the frame is made using beam elements.

*Figure 1. Typical LTB failure of a portal frame structure [2]*

In this work advanced modeling techniques have been developed for analyzing portal frames, with the aim of more precisely evaluating buckling behavior. As this work has been carried out within the PRECASTEEL project, the frame configurations used were based on preliminary calculations carried out by Varelis *et al*. [3].

# 2 Design method according to prEN1993-1-1

According to prEN 1993-1-1 [1], plane structures can be designed to fulfill ULS design criteria by verifying Eq. (1). By this verification buckling is implicitly taken into account.

$$\frac{\chi_{OP} \cdot \alpha_{ult,k}}{\gamma_{M1}} \geq 1 \qquad (1)$$

- $\alpha_{ult,k}$ - is the multiplier of the loads so that the most loaded fibers yield
- $\chi_{OP}$ - the reduction factor due to the non-dimensional slenderness $\lambda_{OP}$
- $\gamma_{M1}$ - safety factor.

The reduction factor $\chi_{OP}$ is related to the non-dimensional slenderness according to the “buckling curves” Figure 6.4 from prEN 1993-1-1. These curves are reproduced in Figure 2. The relationship corresponds to the buckling modes (i.e. lateral buckling, lateral torsional buckling/LTB) that occur in the structure. Because in portal frames, supported out of plane by purlins lateral torsional

buckling is the most significant; this case is discussed according to 6.3.2 of prEN1993-1-1.

## 2.1 Lateral torsional buckling according to prEN 1993-1-1

Using the general methodology, for frames made of welded cross-sections, and a height to width ration larger than 2 (h/b > 2), the curve “d” has to be used. This is the case of most tapered frames, where the h/b ratio exceeds 2, at least in the region of the haunch.

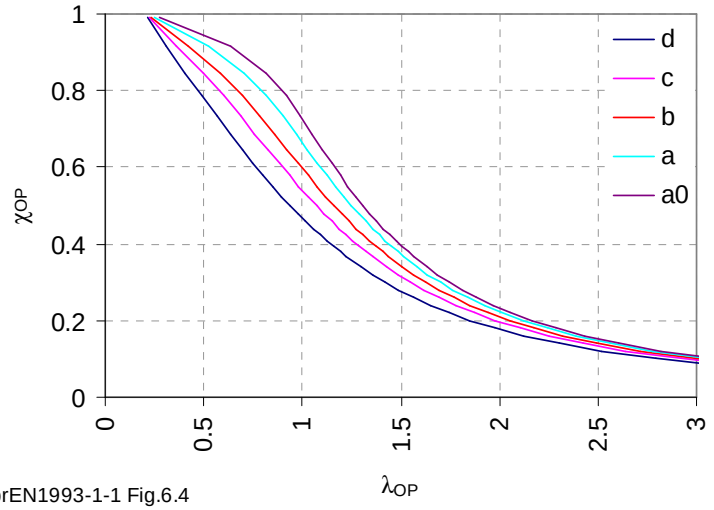


prEN1993-1-1 Fig.6.4

a)

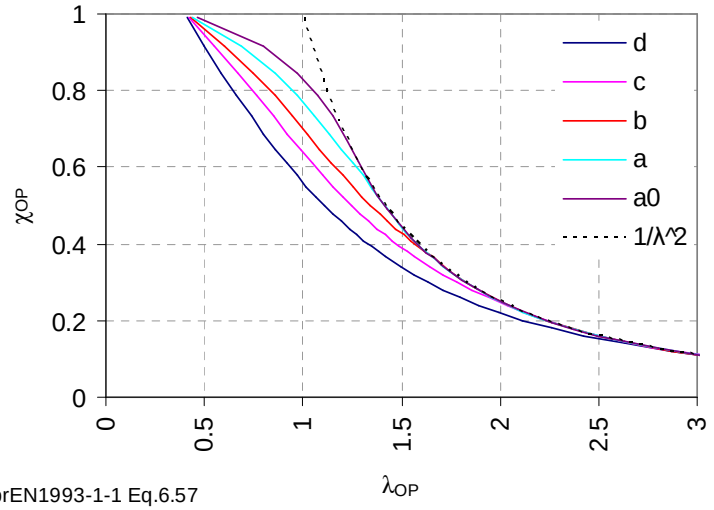


prEN1993-1-1 Eq.6.57

b)

*Figure 2. Buckling curves prEN1993-1-1: (a) Eq.6.56 and (b) Eq.6.57.*

The curves in Figure 2a can be expressed in analytical form by:

$$\chi_{OP} = \frac{1}{\Phi_{OP} + \sqrt{\Phi_{OP}^{\ 2} - \bar{\lambda}_{OP}^{\ 2}}}, \text{ with } \chi_{OP} \le 1,$$

where: $\Phi_{OP} = 0.5 \cdot \left[1 + \alpha_{OP} \cdot \left(\bar{\lambda}_{OP} - 0.2\right) + \bar{\lambda}_{OP}^{\ 2}\right].$

The curves in Figure 2b, can be written as:

$$\chi_{OP} = \frac{1}{\Phi_{OP} + \sqrt{\Phi_{OP}^{\ 2} - \beta \cdot \bar{\lambda}_{OP}^{\ 2}}}, \text{ with } \begin{cases} \chi_{OP} \le 1 \\ \chi_{OP} \le \dfrac{1}{\bar{\lambda}_{OP}^{\ 2}} \end{cases},$$

where: $\Phi_{OP} = 0.5 \cdot \left[1 + \alpha_{OP} \cdot \left(\bar{\lambda}_{OP} - \bar{\lambda}_{OP,0}\right) + \bar{\lambda}_{OP}^{\ 2}\right]$.

In this case prEN 1993-1-1 recommends $\beta = 0.75$ (min) and $\bar{\lambda}_{OP,0} = 0.4$ (max) as most optimistic values to be used with hot-rolled profiles.

In both formulas, $\alpha_{OP}$ is the imperfection factor and its value corresponds to the buckling curve to be used (i.e. a0, a, b, c or d). In case of welded cross-sections with h/b > 2, buckling curve "d" has to be used. As it can be observed from Figure 2.b, curve "d" is not influenced by the use of Eq. 5.57, because it has already been low due to the large imperfection factor ($\alpha_{OP} = 0.76$).

As it is clear from Eq. (1) that $\chi_{OP}$ governs the reduction of loading compared to yielding of the most stressed fiber in the frame, which has to be implemented due to the use of slender elements. If $\chi_{OP}$ is small, this reduction is significant, and the fibers of the frame are very far from yielding at the design loads. E.g. for $\chi_{OP} = 0.5$ and $f_y = 275$ N/mm$^2$, the highest stresses under design loads will be $275 \cdot 0.5 = 137.5$ N/mm$^2$.

The use of very slender elements will lead to the inefficient utilization of the steel in frame. If members are becoming very slender, e.g. for lateral torsional buckling, it is usually possible to provide extra lateral support to the compressed flange in order to reduce slenderness (e.g. Figure 6.5 in prEN1993-1-1). Such supports rarely affect the architectural aspects, as the frames are mainly used in factory or deposit buildings. The only concern is the additional cost.

Therefore, in most applications, it is possible to limit the slenderness so as to obtain a reasonable $\chi_{OP}$ value. E.g. $\chi_{OP} = 0.7$ would mean that, in the most stressed cross-section 70% of the strength of frame is utilized. In this case, the lateral supports for the frame should be arranged so that the slenderness is limited. Following this reasoning, the graphs in Figure 2 can be used reversely, by implying an acceptable reduction factor and determining the required slenderness.

It can be observed that in the range of practical interest for industrial portal frames (i.e. $\chi_{OP} = 0.4 \ldots 0.8$), the two set of curves are quite different, primarily because of the use of the different value for $\bar{\lambda}_{OP,0}$ (i.e. 0.2 in Eq. 6.56 and 0.4 in Eq.6.57). The selected curves "a" & "d: are presented comparatively from Eq. 6.56 and Eq. 6.57 in Figure 3.

Unfortunately, prEN 1993-1-1[1] is not clear about which of the two curves (i.e. based on Eq. 6.56 or Eq.6.57) should be used for portal frames (These frames are affected mostly by LTB, as it will be seen later). In the following analysis, the more conservative curve based on Eq. 6.56 will be used. It should be noted that the use of Eq.6.57 could lead to substantially lower reduction factor, and higher predicted capacity of the frames.

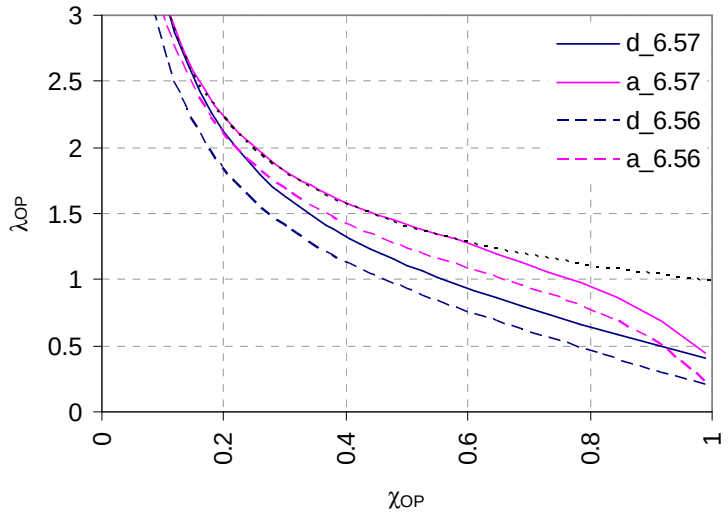


*Figure 3. Slenderness vs. reduction factor $\chi_{OP}$.*

The evaluation of $\lambda_{OP}$ should be done according to the Eq. 6.64 of prEN1993-1-1, reproduced in Eq. (2) below:

$$\lambda_{OP} = \sqrt{\frac{\alpha_{ult,k}}{\alpha_{cr,OP}}} \qquad (2)$$

Where: $\alpha_{ult,k}$ is the multiplier of the loads so that the most loaded fibers yield
$\alpha_{cr,OP}$ is the multiplier of the loads for reaching the critical load (1st buckling).

## 2.2 Application of the EN1993-1-1 design method

In Example 1 (1.2 - Version 1) a frame with height of H = 6m and span of 20m has been considered. The first design attempt was made with sections: 200…800…400×180×8×8 ($h_{base}$...$h_{haunch}$_$h_{beam}$×Width×$t_{flange}$×$t_{web}$). At first, the uniformly distributed vertical load is chosen as $P_{des}$=100 N/m$^2$.

The following values were obtained from the FEM model presented in Figure 4:
$\alpha_{cr,OP}$ = 13.65 (lateral torsional buckling - Figure 4a)
$\sigma_{max}$ = 8.96 N/mm$^2$ (on inner flange of the column at haunch - Figure 4b) → $\alpha_{ult,k}$ = 275/8.96 = 30.69.

Therefore: $\lambda_{OP}$ = sqrt($\alpha_{ult,k}/\alpha_{cr,OP}$) = sqrt(30.69/13.65) = 1.50. This slenderness results in a reduction factor $\chi_{OP}$ = 0.28, which means that in terms of strength 28% of the frame is utilized. The frame is very slender. When the loading is increased to the real distributed load $P_{des}$ = 1640 N/m$^2$, than the yield load multiplier is $\alpha_{ult,k}$ = 100/1640×30.69 = 1.87, and the buckling multiplier $\alpha_{cr,OP}$ = 100/1640×13.65 = 0.83 is obtained. As $\alpha_{cr,OP}$ < 1, it means that this structure would buckle at 83% of $P_{des}$ = 1640 N/m$^2$.

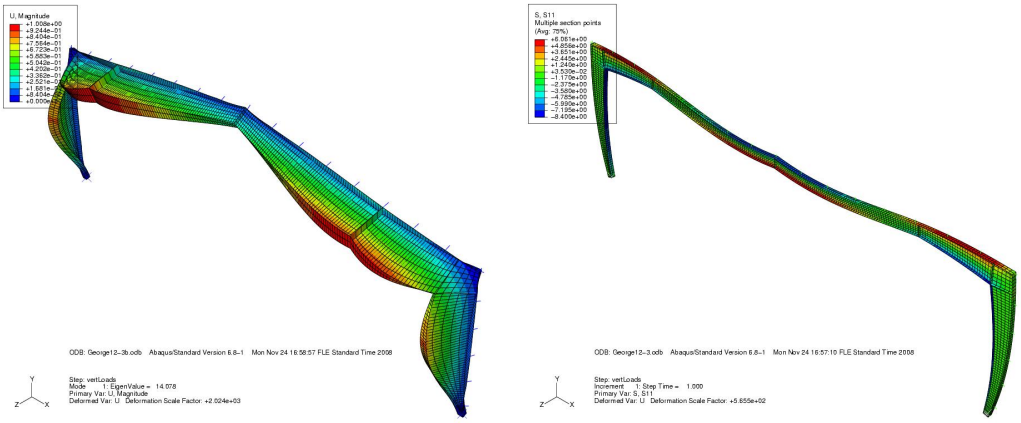

a) b)

*Figure 4. Results of buckling & elastic analysis of the frame.*

In order to reduce the slenderness of the initial frame, one can attempt to block buckling of the inner flange at the frame corner. This is a very common technique and it presumes the placing of a blocking from the purlins to support the compressed flange.

The result can be seen in Figure 5a. The critical load multiplier ($\alpha_{cr,OP}$) has increased from 0.83 to 1.84, and the $\lambda_{OP}$ = 1.01. The corresponding reduction factor is $\chi_{OP}$ = 0.46.

The buckling behavior can be improved further by supplying additional torsional support at the end of the variable section of the beam. The critical load is now $\alpha_{cr,OP}$ = 2.09, and the $\lambda_{OP}$ = 0.95. The corresponding reduction factor is $\chi_{OP}$ = 0.49. In order to improve the buckling performance even more, one should provide torsional restraint to the compressed flange of the column, a solution which is less widely used, because it reduces the useful space inside the hall.

This last solution with two torsional supports fulfills ULS design requirements for vertical distributed load up to $P_{DIST}$, according to the calculation below:

$$\frac{\chi_{OP}\cdot\alpha_{ult,k}}{\gamma_{M1}}\le 1\Rightarrow \frac{\chi_{OP}\cdot\dfrac{\alpha_{ult,k}\cdot P_{1640N/m^2}}{P_{DIST}}}{\gamma_{M1}}\le 1\Rightarrow \tag{3}$$

$$P_{DIST}\le\frac{\chi_{OP}}{\gamma_{M1}}\cdot\alpha_{ult,k}\cdot P_{1640N/m^2}\Rightarrow P_{DIST}\le\frac{\chi_{OP}}{\gamma_{M1}}\cdot P_{yield}$$

$$P_{DIST}\le\frac{0.49}{1.1}\cdot 1.87\cdot 1640N/m^2=1.37kN/m^2.$$

It can be noted that $P_{yield}=1.87\cdot 1640=3067kN/m^2$ represents the distributed load at which yielding of the most stressed fiber occurred, when not taking into account out of plane deformations.

As mentioned earlier, the ULS design load for this frame is $P_{des}$ = 1640N/mm$^2$; resulting from the load combination "1.35 · Permanent loads + 1.5 · Variable loads" [4] (i.e. $P_{des}$ = 1.35 · 0.38 + 1.5 · 0.75 = 1.64 kN/m$^2$), plus the self-weight

of the frame. In the above calculation, the nominal value of the weight of the roof (e.g. purlins, sheeting, thermal insulation, lighting, ducts, etc.) is 0.38N/m$^2$, and the nominal snow load is 75N/m$^2$.

Therefore, this configuration will not fulfill the design requirements if Eq. 6.56 (prEN1993-1-1) is used for calculating LTB. Even if the more favorable buckling criteria according to e.g. Eq 6.57 (prEN1993-1-1) is used; then $\chi_{OP}$ = 0.58, and:

$$P_{DIST} \le \frac{0.58}{1.1} \cdot 1.87 \cdot 1640 \text{N/m}^2 = 1.62 \text{kN/m}^2 .$$

One more observation refers to the self-weight of the frames, which play a role in the calculations and may not be neglected. However, in this study gravity has been neglected, and hence frames have no mass (and weight) in the models. For example, the net/FEM mass of the frame in Figure 5 is M = 1689 kg, which corresponds to a distributed mass of $P_M$ = M·g/(Span·Distance) = 1689·g/(20·6) ~ 0.14 kN/m$^2$. If this distributed load is considered to act on the beams, which is a quite conservative assumption, then $P_{DIST}$ should be decreased with $P_M$, and the distributed load excluding self-weight that can be resisted by the frame is $P_{ULS}$ = $P_{DIST}$ - $P_M$ = 1.37 - 0.14 = 1.23 kN/m$^2$. This value has to compared with the distributed design load $P_{des}$ = 1.64 kN/m$^2$.

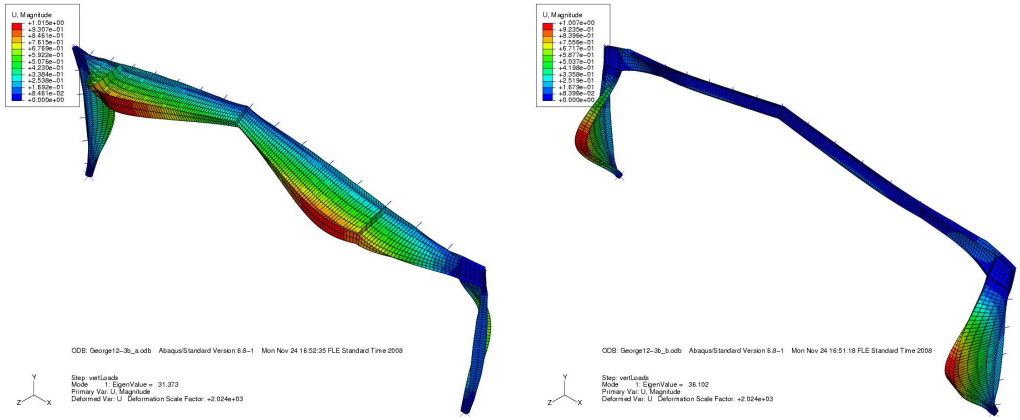

a) b)

*Figure 5. Buckling results with supplementary supports.*

It should be noted that the cross-sections have been constructed so that the profiles stay close to Class 3 (actually they both resulted Class 4):

- web: (800 - 2 · 8 - 2 · 4)/8 = 97 (limit in Table 5.2 prEN 1993-1-1 c/t = 42·ε/(0.67 + 0.33 · ψ) ~ 91 → web Class 4)

- flange: ((180 - 8 - 2 · 4)/2)/8 = 10.25 (limit in Table 5.2 prEN 1993-1-1 c/t = 14 · ε ~ 12.88 → flange Class 3)

Details of this configuration are given in the table in Appendix A under the name 1.2-1c.

# 3 Effects of the purlin support on the stability of frames

Unless other connecting elements are provided in the longitudinal direction of the hall (e.g. longitudinal bracing ties, eaves beam or tie etc.); purlins alone provide lateral support to the frames. The effectiveness of this support depends on the type of the purlin and its fixing to the frame.

In the following section, it is supposed that light-gauge steel (LGS) purlins are used and that other connections are not provided between the frames. For simplicity, a typical configuration of frame and purlin is studied, in order to obtain the magnitude of the stabilizing forces given by the purlins.

The use of light-gauge Z purlin is proposed as purlins. Such purlins are very common and are produced by several major steel producers (e.g. Lindab, Konti, Ruukki, etc.). For the example the Z purlin in Figure 6 was used, combined to a frame distance of T = 6 m. 150 mm is a common height for roof purlins in order to resist snow load, and accommodate the thermal insulation. The purlin used in this particular example is a Z150/2 produced by Lindab.

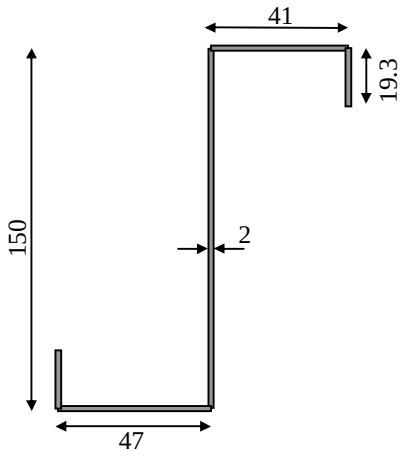


*Figure 6. Z150/2 purlin.*

The purlin is supposed to be connected to the frame as represented in Figure 7a. This means that the frame in the connection point will have (i) a lateral and (ii) a torsional support. Further, the (iii) configuration in Figure 7b can be used to provide lateral support to the lower flange of the frame element (e.g. recommended by prEN1993-1-1, Figure 6.5 [1]).

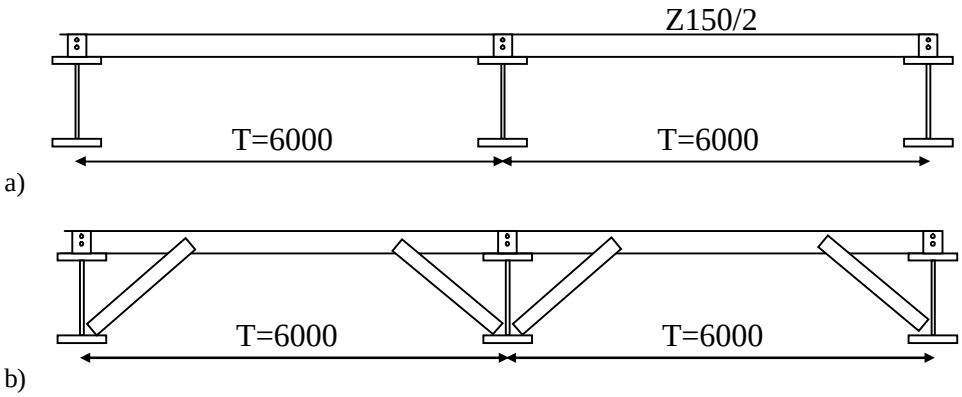


*Figure 7. Connection to purlins to the frame.*

In the following section, the efficiency (i.e. supporting stiffness) of these types of support is evaluated. The following section is based on similar considerations as discussed in prEN1993-1-3 [6], "§10.1 – Beams restrained by sheeting", dealing with LGS purlins supported against buckling by trapezoidal sheeting.

The stiffnesses provided to the different parts of the frame cross-section are presented in Figure 8. The tension flange is laterally supported with a translational stiffness $K_{tf}$, and a rotational stiffness $K_t$. The blockings connecting the compressed flange (Figure 7b), provide a translational support $K_{cf}$.

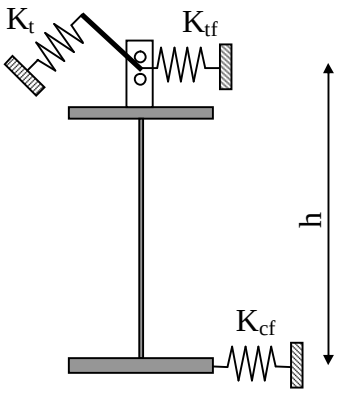


*Figure 8. Stiffness from purlin to frame.*

In order to evaluate $K_t$, and $K_{tf}$, the micro modeling from Figure 9 is proposed. In these models, $K_b$ is the stiffness of the bolted connection of the purlin, while $K_{ax}$ and $K_{be}$ are the axial and bending stiffness of the purlin respectively. The slider $S_b$ takes into account the possibility that the bolted connections, subjected to shear, can slip in the initial loading stage.

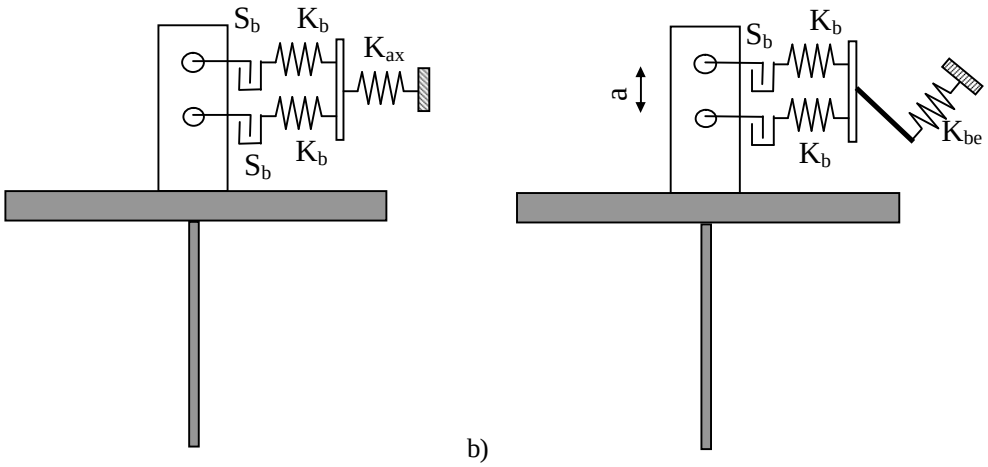


*Figure 9. Components of $K_t$ and $K_{tf}$ on the micro scale.*

The models presented in Figure 10 have been used to determine the rigidities of the purlins. With the Z150/2, the values of $K_{be}$ = 1/0.00269 = 372 kNm/rad, $K_{ax}$ = 1/0.027 = 37 kN/mm and $K_{cf}$ = 1/1.171 = 0.85 kN/mm have been obtained.

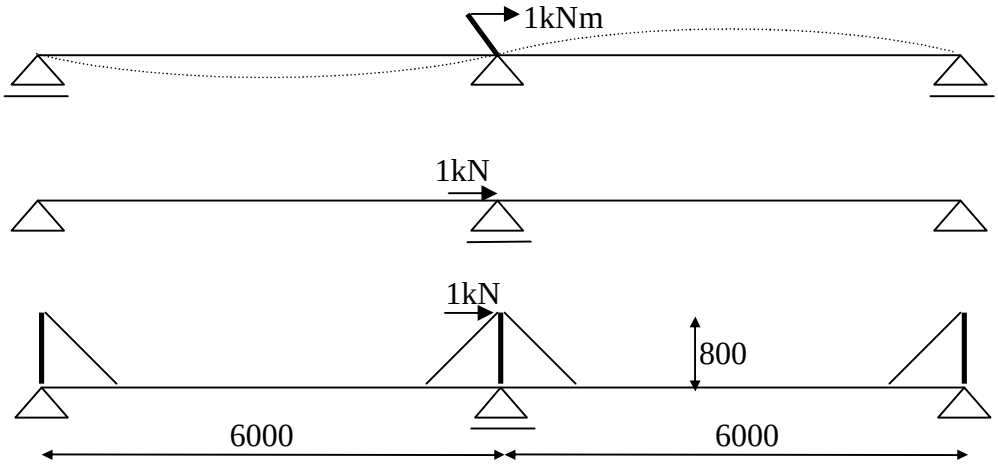


*Figure 10. Models for determining the stiffness of purlins.*

These values can be determined analytically if the purlins are supposed to have constant cross-section in both spans and spans are equal:

$$K_{ax} = \frac{2 \cdot E \cdot A}{L} \qquad (4)$$

$$K_{be} = \frac{6 \cdot E \cdot I}{L}$$

Where: E is the modulus of elasticity of the purlin material (normally steel)
A the cross-section area of the purlin
I the second moment of area of the purlin corresponding to the axis of bending
L the length of the two purlin segments.

The values of $K_b$ can be calculated using the formulation proposed by Zaharia [8]. Both $K_b$ for a single bolt connection and the rotational stiffness for a double bolt connection were developed and calibrated based on test [9]. The proposed expression for the stiffness of one bolt connection is:

$$K_b = 6.8 \cdot \frac{\sqrt{D}}{\frac{5}{t_1} + \frac{5}{t_2} - 1} \text{(kN/mm)} \qquad (5)$$

Where: D is the diameter of the bolt
$t_1$ & $t_2$ is the thicknesses of the two connected steel plates.

If this bolt stiffness is presumed we have the following expression for $K_{ft}$ and $K_t$:

$$K_{ft} = \frac{1}{\frac{1}{K_{ax}} + \frac{1}{2 \cdot K_b}} \qquad (6)$$

$$K_t = \frac{1}{\frac{1}{K_{be}} + \frac{1}{K_{b\_rot}}}, \text{ where } K_{b\_rot} = \frac{a^2 \cdot K_b}{2}$$

In the example case of using Z150/2 profiles as purlins, and some type of usual U profile for the supports, $t_1$ = 5 mm and $t_2$ = 2 · 2 = 4 mm can be presumed. $t_2$ is doubled because there is usually an overlapping portion of the purlin over the support. It is also usual to use M12 bolt for these types of connections. For these parameters the value $K_b$ = 18.8 kN/mm is obtained. The value of *a* (Figure 9) is strongly influencing the rotational stiffness of the connection, and $K_t$ (eq.(6)) depends very much on it. Usual value in practice is a = 35mm, but for the Z150/2 profile the largest possible value is about a = 100 mm. For this later case, the value of $K_{ft}$ = 18.7 kN/mm and $K_t$ = 75.2 kNm/rad are obtained. The values for a = 35 mm, more typical in practice would be $K_{ft}$ = 18.7 kN/mm and $K_t$ = 11.2 kNm/rad.

An other property of the bolted connection of the purlin is the magnitude of the possible slip ($S_b$ - Figure 9), because bolt holes are drilled with certain tolerance. Dubina [9] reported that holes for the M12 bolts were drilled to diameter of 13 mm, for the test specimens used to calibrate the expression for $K_b$ and the derived expression of $K_{b\_rot}$.

When subjected to axial loading during test, single-bolt lap joints showed a slip of about 2 mm [8]. In these cases the threaded part of the bolt came in contact with the bolt-hole. In bending experiments a rotation slip of $\Phi_{ini}$ = 0.02…0.11 rad, with an average value of 0.076 rad [9] has been observed. The scatter of the rotational test results is very big. As a thumb rule the slip rotation values approximately correspond to $\Phi_{ini}$ = arctan(2/a) = 0.02 rad (for a = 100 mm), which is the rotation of the connection at the consummation of the 1mm slip in both bolts. During the slip the force or bending moment is very small, and the stiffness can be considered 0 (Figure 11).

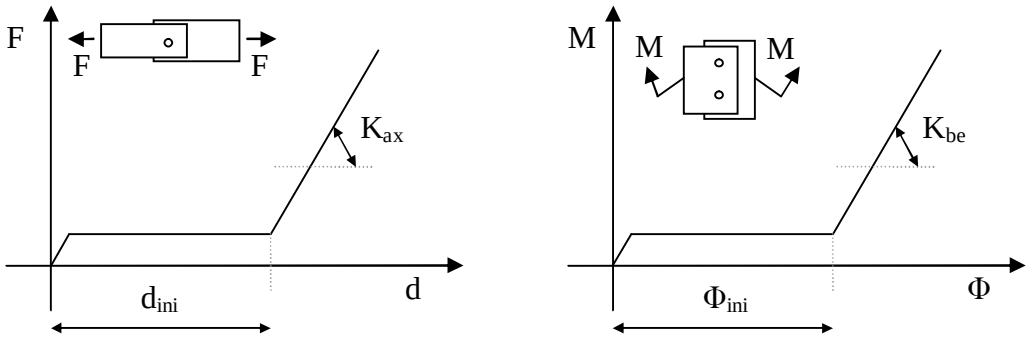


*Figure 11. Axial and rotational behavior of the bolted connection fixing the purlin.*

It is also very important to note, that at for the slip-rotation levels correspond to a quite large torsional deformation at the level of the cross-section (Figure 12). E.g. for a H = 120 + 600 mm height, the lower flange of the profile should have a

displacement of $d_\Phi$ = 14.4 mm, corresponding to the $\Phi_{ini}$ = 0.02 rad discussed above for Z150/2 purlins.

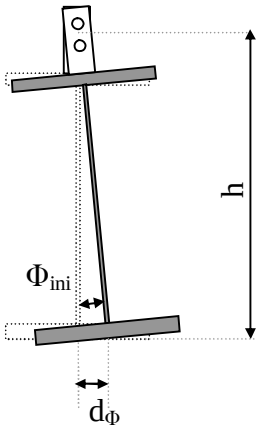


*Figure 12. Axial and rotational behavior of the bolted connection fixing the purlin.*

The *Frame 1.2-3b*, from Appendix A, was analyzed with the different lateral support conditions presuming the use of Z150/2 profiles. The analyzed cases are and results are summarized in Table 1. It should be noted that results in Table 1 neglect the possibility of slip in the connection.

*Table 1. Frame 1.2-3b with different support conditions.*

| | **Geometry** | | | | | | | | | **Restraint** | | | | | | | | |
|---|---|---|---|---|---|---|---|---|---|---|---|---|---|---|---|---|---|---|
| | **S** | **T** | **$h_c$** | **$h_h$** | **$h_b$** | **b** | **$t_f$** | **$t_w$** | **a** | **$K_{ft}$** | **$K_t$** | **$K_{cf}$** | **$\lambda_{OP}$** | **$\chi_{OP-1}$** | **$\alpha_{cr,OP}$** | **$\alpha_{ult,k}$** | **$\sigma_{max}$** | **$P_{DIST}$** |
| Type | (m) | (m) | (mm) | (mm) | (mm) | (mm) | (mm) | (mm) | (mm) | (N/mm) | (Nmm/rad) | (N/mm) | | | | | (N/mm$^2$) | (kN/m$^2$) |
| | | | | | | | | | | $P_{des}$ = 1.64 kN/m$^2$ | | | | | | | | |
| 1 | | | | | | | | | | ∞ | 0 | 0 | 1.00 | 0.47 | 2.31 | | | 1.61 |
| 2 | | | | | | | | | | 18700 | 0 | 0 | 1.00 | 0.47 | 2.30 | | | 1.61 |
| 3 | | | | | | | | | 100 | ∞ | 75150000 | 0 | 0.85 | 0.55 | 3.22 | | | 1.90 |
| 4 | | | | | | | | | 100 | 18700 | 75150000 | 0 | 0.85 | 0.55 | 3.21 | | | 1.90 |
| 5 | | | | | | | | | 35 | ∞ | 11200000 | 0 | 0.92 | 0.51 | 2.76 | | | 1.77 |
| 6 | | | | | | | | | 35 | 18700 | 11200000 | 0 | 0.92 | 0.51 | 2.75 | | | 1.76 |
| 7 | 20 | 6 | 200 | 800 | 400 | 240 | 10 | 8 | | ∞ | ∞ | 0 | 0.82 | 0.57 | 3.47 | 2.31 | 119 | 1.96 |
| 8* | | | | | | | | | | ∞* | ∞* | 0 | 0.79 | 0.58 | 3.67 | | | 2.01 |
| 9 | | | | | | | | | | ∞ | 0 | ∞ | 0.69 | 0.65 | 4.83 | | | 2.24 |
| 10 | | | | | | | | | | ∞ | 0 | 850 | 0.87 | 0.54 | 3.06 | | | 1.85 |
| 11 | | | | | | | | | | 18700 | 0 | 850 | 0.87 | 0.54 | 3.05 | | | 1.85 |
| 12 | | | | | | | | | 35 | 18700 | 11200000 | 850 | 0.82 | 0.57 | 3.45 | | | 1.96 |
| 13 | | | | | | | | | | ∞ | ∞ | ∞ | 0.59 | 0.72 | 6.67 | | | 2.47 |

NOTE: * The purlin support has been increased from I50…50x3x3 to I100…100x3x3

The values of $\alpha_{cr,OP}$ in Table 3 lead to a few important conclusions:

- The lateral (out of plane translational) support given by the purlins seam to be effective even when provided by the thin walled Z150/2 purlin (compare cases 1 & 2, 3 & 4, 4 & 6, 10 & 11).

- Torsional support at the purlin connection would be a very effective way of reducing slenderness of the frames (e.g. 1 & 3, 1 & 5, 11 & 12). However the effect is very much influenced by such minor details as distance between bolts (3 & 5), stiffness of the purlin supporting strut (7 & 8). Noting that the rotational slip in the bolted connection might allow a significant initial rotation in the bolted connection, raises serious questions on the reliability of this torsional restraint.
- The lateral support of the corner of the frame as in Figure 7 seam to be less efficient than full support because of the bending flexibility of the purlin (9 & 10). This is worrying because prEN1993-1-1 explicitly mentions this as solution to provide torsional support to the frame. The efficiency of the lateral support can be increased if the bending capacity of the purlin is increased or a different scheme is adopted for the supporting elements (Figure 13).

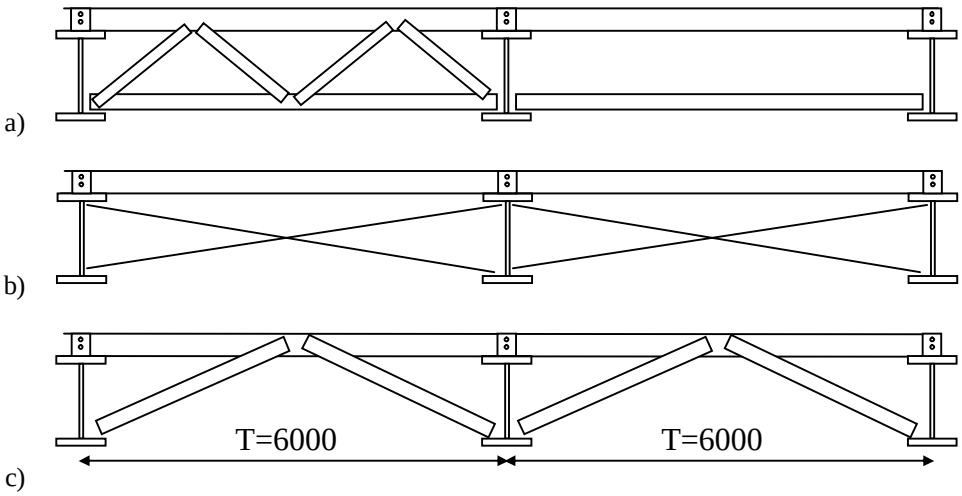


*Figure 13. Connection to purlins to the frame.*

The stiffnesses ($K_{cf}$) with arrangements of Figure 13 are: $K_{cf-a}$ = 1/0.039 kN/mm (all elements Z150/2), $K_{cf-b}$ = 1/0.262 kN/mm (Φ = 12 mm), and $K_{cf-c}$ = 1/0.367 kN/mm (all elements Z150/2). As it can be seen in Table 2, only configurations Figure 13a and Figure 13b provide lateral support comparable with the theoretical $K_{cf-b} = \infty$ case.

*Table 2. Frame 1.2-3b with corner support of different types.*

| | Geometry | | | | | | | | Restraint | | | | | | | | |
|---|---|---|---|---|---|---|---|---|---|---|---|---|---|---|---|---|---|
| | **S** | **T** | **$h_c$** | **$h_h$** | **$h_b$** | **b** | **$t_f$** | **$t_w$** | **$K_{ft}$** | **$K_t$** | **$K_{cf}$** | **$\lambda_{OP}$** | **$\chi_{OP-1}$** | **$\alpha_{cr,OP}$** | **$\alpha_{ult,k}$** | **$\sigma_{max}$** | **$P_{DIST}$** |
| Type | (m) | (m) | (mm) | (mm) | (mm) | (mm) | (mm) | (mm) | (kN/mm) | (kNm/rad) | (kN/mm) | | | | | (N/mm2) | (kN/m2) |
| | | | | | | | | | $P_{des}$ = 1.64 kN/m$^2$ | | | | | | | | |
| 9 | | | | | | | | | ∞ | 0 | ∞ | 0.69 | 0.65 | 4.83 | | | 2.24 |
| 9a | 20 | 6 | 200 | 800 | 400 | 240 | 10 | 8 | ∞ | 0 | 25641 | 0.69 | 0.65 | 4.83 | 2.31 | 119 | 2.24 |
| 9b | | | | | | | | | ∞ | 0 | 3817 | 0.70 | 0.64 | 4.70 | | | 2.21 |
| 9c | | | | | | | | | ∞ | 0 | 2725 | 0.74 | 0.62 | 4.24 | | | 2.13 |

Based on these results it is concluded that, unless the purlins are (i) much stiffer in bending than the light-gauge Z150/2 discussed here and (ii) the slip in the fixing of the purlin connection is prevented:

- It is not reliable to account on the rotational support of the purlin fixings. It is possible and probably economical to develop stiff fixings.
- It is reasonable to model the lateral support given by purlins with ∞ stiffness.
- It is feasible to model corner fixing as $K_{cf\text{-}b} = \infty$, but only if Figure 13.a or b typologies are used.

Buckling modes of the frames from Table 1 & Table 2 are presented in Figure 14.

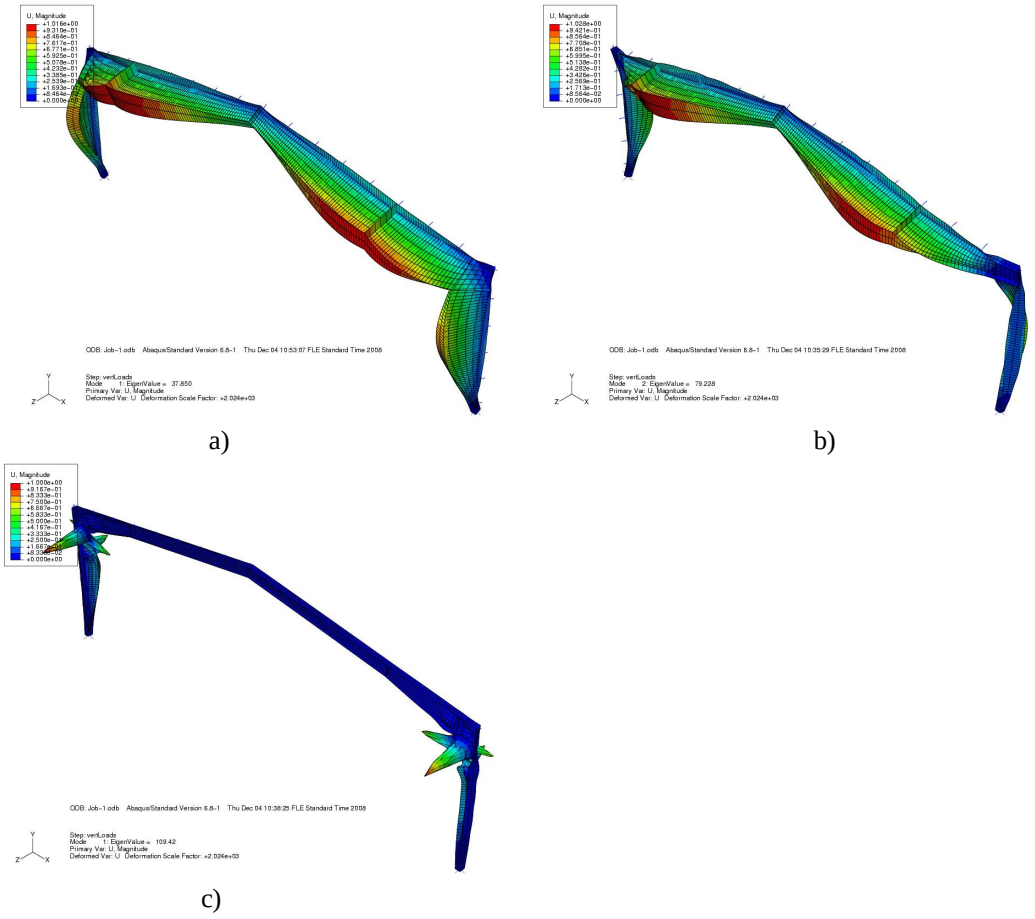

*Figure 14. Buckling shapes of 1.2-3b frames: a) 1 to 8, 10 to 12, 9-b & 9-c, b) 9, 9-a, c) 13.*

# 4 Parametric study

## 4.1 Elastic analysis with the procedure described in Ch.2

### 4.1.1 Check for ULS combination of vertical loads

The procedure described in Ch. 2.1, and tested in Ch. 2.2, has been applied to the frame configurations proposed for detailed examination (Table 3). The design was

only concentrating on the vertical loads ($ULS_V$). A few alternative configurations have been analyzed:

- the frame made of hot-rolled sections
- the frame made of built-up tapered sections without the use of any torsional restraint
- the frame made of built-up tapered sections and using torsional restraints. Torsion restraint was provided in the corner of the frame (C), or both in the corner and the end of the taper in the beam (C + T). The torsional restraint in these points was considered with ∞ stiffness (see conclusions of Ch. 3).

*Table 3. Design alternatives for detailed design of frames.*

| | | **S** (m) | **T** (m) | **$P_{des}$** (kN/m$^2$) | **$h_c$** (mm) | **$h_h$** (mm) | **$h_b$** (mm) | **b** (mm) | **$t_f$** (mm) | **$t_w$** (mm) | Torsional restraint | **$\lambda_{OP}$** | **$\chi_{OP-1}$** | **$\alpha_{cr,OP}$** | **$\alpha_{ult,k}$** | **$\sigma_{max}$** | **$P_{DIST}$** (kN/m$^2$) | **$M_{fr}$** (kg) | **$P_{ULS}$** (kN/m$_2$) |
|---|---|---|---|---|---|---|---|---|---|---|---|---|---|---|---|---|---|---|---|
| 1.2-O | | 20 | 6 | 1.64 | | HEA300, IPE360 | | | | | - | 0.76 | 0.75 | 2.22 | 1.29 | 213 | 1.44 | 2412 | 1.24 |
| 2.2-O | | | | | | HEA300, IPE330 | | | | | - | 0.86 | 0.69 | 1.65 | 1.21 | 227 | 1.24 | 2215 | 1.06 |
| 1.2-2 | c | | | | 200 | 800 | 400 | 220 | 8 | 8 | C+T | 0.73 | 0.62 | 3.59 | 1.90 | 144 | 1.77 | 1855 | 1.62 |
| 1.2-4 | a | | | | 200 | 800 | 400 | 260 | 10 | 8 | - | 0.93 | 0.51 | 2.87 | 2.46 | 112 | 1.86 | 2291 | 1.67 |
| 3.6-O | | 32 | 6 | 2.76 | | HEA650, IPE600 | | | | | - | 0.99 | 0.60 | 1.32 | 1.29 | 213 | 1.96 | 7051 | 1.59 |
| 3.6-4 | b | | | | 300 | 1200 | 500 | 380 | 14 | 12 | C+T | 0.59 | 0.71 | 4.42 | 1.56 | 176 | 2.79 | 6458 | 2.46 |
| 3.6-3 | a | | | | 350 | 1400 | 600 | 400 | 14 | 10 | - | 0.77 | 0.60 | 3.29 | 1.93 | 142 | 2.91 | 6628 | 2.57 |
| 2.8-O | | 20 | 6 | 1.64 | | HEA320, IPE330 | | | | | - | 0.86 | 0.68 | 1.64 | 1.23 | 224 | 1.25 | 2711 | 1.03 |
| 2.8-3 | a | | | | 240 | 960 | 400 | 260 | 10 | 8 | - | 1.11 | 0.42 | 2.40 | 2.94 | 93 | 1.82 | 2711 | 1.60 |
| 3.20-O | | 16 | 6 | 2.76 | | HEA340, IPE360 | | | | | - | 0.70 | 0.78 | 2.87 | 1.42 | 194 | 2.78 | 2355 | 2.53 |
| 3.20-1 | b | | | | 200 | 800 | 400 | 220 | 8 | 8 | C | 0.76 | 0.60 | 3.10 | 1.81 | 152 | 2.73 | 1625 | 2.56 |
| 3.20-2 | a | | | | 200 | 800 | 400 | 240 | 10 | 8 | - | 0.93 | 0.50 | 2.52 | 2.19 | 125 | 2.76 | 1917 | 2.56 |

The results of the study are summarized in Table 3, while a detailed table with all analyzed configurations is presented in Appendix A. It can be noted that frames 2.2 and 2.8 have been designed for low snow loads (i.e. $P_{des}$= 1.35 × 0.38 + 1.5 × 0.75 = 1.64 kN/m$^2$), while frames 3.6 and 3.20 for high snow load (i.e. $P_{des}$ = 1.35 × 0.38 + 1.5 × 1.50 = 2.76 kN/m$^2$). The values of $\alpha_{cr,OP}$, $\alpha_{ult,k}$ and $\sigma_{max}$, all presented for the respective values of $P_{des}$, result from the FEM analysis. $\alpha_{cr,OP}$ is used to determine the slenderness of the frame ($\lambda_{OP}$). The reduction factor $\chi_{OP}$ is determined from the buckling curve "b" (Eg.6.56 in prEN1993-1-1) in case of hot-rolled profile frames and from curve "d" (Eq.6.56) in case of welded frames. The maximum load capacity of the frame ($p_{ULS}$) was then calculated using Eq. (3).

It is interesting to note that configurations 1.2, 3.6 and 2.8 are underdesigned according to the pre-design ($P_{ULS} < P_{des}$). This may be because of the difficulty of accounting for the lateral torsional buckling of variable cross-section members. In any case, for these configurations, a further increase of the cross-sections seems to be necessary.

By using welded frames, the steel consumption can be reduced by about 5%, if no torsion restraints are added (see 2.2 & 3.6). If torsion restraints are added, the welded solution can be 20% lighter than the hot-rolled one (also 2.2). This

reduction is possible together with the change of support condition from fixed (hot-rolled) to pinned (welded). The change of support will also result in reduction of the dimensions of the foundation. The disadvantage of the welded solutions is the higher fabrication cost, and technological difficulties, of producing the elements.

In case of configuration 2.8 the gain is less because of the height of the frame (8 m). In this case, the release of the base fixing increases the buckling length of the frame. The solution with torsion support in the corner is also not efficient for this configuration, because the failure mode is LTB of the column. An efficient solution in this case would be to provide torsion restraint to the column at mid-height, but this was not investigated. Without the torsion support at the mid-height of column, the fixed based frame appears to be very competitive, because the slenderness of the frame remains within reasonable limits.

The gain in case of frame 3.20 is more significant than the 10% and 20% previously observed, primarily because the hot-rolled frame was already pinned. It should also be observed that 3.20 was the only case which, in it's original configuration fulfilled the design requirement.

### 4.1.2 Check for ULS combination of earthquake loads

The frames configured for vertical loads only are analyzed considering the effect of the earthquake, with $a_g$ = 0.32g, Type 1 spectra on Soil B. The earthquake loading was taken into account as equivalent horizontal loads at the corner of the frames, generated by the mass of the frame ($M_{fr}$ - Table 3) multiplied by 1.4, and the load from the cladding (0.38 kN/m$^2$). The mass of the frame obtained from ABAQUS was increased by 40% in order to take into account additional plates and bolts that were not included in the model.

Therefore, two vertical loads were acting on the frame: (i) 1.4 × $M_{fr}$ recalculated to weight and (ii) 6 × 0.38 kN/m$^2$, (T = 6 m is the distance between two frames, 0.38 self-weight of sheeting). These forces were considered distributed on the roof only ($P_{ULS-EQ}$).

Complementarily, the earthquake generated equivalent horizontal forces ($F_H$) were acting on the frame corresponding to the earthquake mass $M_{EQ}$ = 1.4 × $M_{fr}$ + 6 × S × 38 kg. In order to determine the equivalent horizontal forces, first the lateral rigidity ($K_H$) of the frame has been calculated, and then the period of vibration ($T_1$) using $M_{EQ}$. The spectral acceleration corresponding to $T_1$ has been extracted from the elastic spectra ($a_g$ = 3.2 m/s$^2$, Type 1, Soil B) and the horizontal force $F_H$ calculated (i.e. this is the "Lateral force method of analysis" from EN1998-1 [7]).

$P_{ULS-EQ}$ was applied to the frame in an initial load step; then $F_H$ was used in a second step for two types of analysis: (i) buckling analysis, to determined the multiplier $\alpha_{cr,OP}$ of the load $F_H$, and (ii) incremental analysis to determine the multiplier $\alpha_{ult,k}$ of $F_H$ to produce yielding (i.e. yielding when buckling is prevented). The design check is carried out using Eq. (1).

The results of these analyses are presented in Table 4.

*Table 4. Check for EQ loads in ULS considering PGA = 0.32 g.*

| | S (m) | T (m) | $h_c$ (mm) | $h_h$ (mm) | $h_b$ (mm) | b (mm) | $t_f$ (mm) | $t_w$ (mm) | $M_{EQ}$ (kg) | $K_H$ (kN/m) | $T_1$ (s) | $S_{e1}$ ($m/s^2$) | $F_H$ (kN) | $\sigma_{max}$ ($N/mm^2$) | $\alpha_{cr,OP}$ | $\alpha_{ult,k}$ | $\lambda_{OP}$ | $\chi_{OP-1}$ | Check |
|---|---|---|---|---|---|---|---|---|---|---|---|---|---|---|---|---|---|---|---|
| 1.2-O | | | | HEA300, IPE360 | | | | | 7937 | 2521.2 | 0.35 | 9.6 | 76.2 | 174.5 | 2.69 | 1.86 | 0.83 | 0.70 | 1.19 |
| 2.2-O | 20 | 6 | | HEA300, IPE330 | | | | | 7661 | 2225.2 | 0.37 | 9.6 | 73.5 | 180.7 | 2.19 | 1.79 | 0.90 | 0.66 | 1.07 |
| 1.2-2 | c | | 200 | 800 | 400 | 220 | 8 | 8 | 7157 | 886.6 | 0.56 | 8.51 | 60.9 | 160.7 | 3.53 | 1.94 | 0.74 | 0.62 | 1.09 |
| 1.2-4 | a | | 200 | 800 | 400 | 260 | 10 | 8 | 7767 | 1181.4 | 0.51 | 9.43 | 73.2 | 139.9 | 2.07 | 2.27 | 1.05 | 0.44 | 0.92 |
| 3.6-O | | | | HEA650, IPE600 | | | | | 17167 | 17013.6 | 0.20 | 9.6 | 164.8 | 124.6 | 4.41 | 3.16 | 0.85 | 0.70 | 2.00 |
| 3.6-4 | b | 32 6 | 300 | 1200 | 500 | 380 | 14 | 12 | 16337 | 3048.6 | 0.46 | 9.6 | 156.8 | 140 | 7.54 | 2.36 | 0.56 | 0.74 | 1.58 |
| 3.6-3 | a | | 350 | 1400 | 600 | 400 | 14 | 10 | 16575 | 4537.1 | 0.38 | 9.6 | 159.1 | 116 | 4.2 | 2.97 | 0.84 | 0.56 | 1.50 |
| 2.8-O | | | | HEA320, IPE330 | | | | | 8355 | 1213.8 | 0.52 | 9.21 | 77.0 | 195.2 | 1.58 | 1.57 | 1.00 | 0.60 | 0.85 |
| | 20 | 6 | | | | | | | | | | | | | | | | | |
| 2.8-3 | a | | 240 | 960 | 400 | 260 | 10 | 8 | 8355 | 750.7 | 0.66 | 7.25 | 60.6 | 157.7 | 1.91 | 2.03 | 1.03 | 0.45 | 0.83 |
| 3.20-O | | | | HEA340, IPE360 | | | | | 6945 | 782.9 | 0.59 | 8.12 | 56.4 | 164 | 2.07 | 2.22 | 1.04 | 0.57 | 1.16 |
| 3.20-1 | b | 16 6 | 200 | 800 | 400 | 220 | 8 | 8 | 5923 | 1059.7 | 0.47 | 9.6 | 56.9 | 143.2 | 2.63 | 2.16 | 0.91 | 0.52 | 1.01 |
| 3.20-2 | a | | 200 | 800 | 400 | 240 | 10 | 8 | 6332 | 1326.6 | 0.43 | 9.6 | 60.8 | 120.7 | 2.81 | 2.62 | 0.97 | 0.49 | 1.15 |

It can be noted from Table 4, that the frames designed previously only for vertical loads all satisfy the horizontal (earthquake ULS requirements), except in the case of the Frames 2.8; which have a height of H = 8 m, span of S = 20 m and reduced snow load (0.75 $kN/m^2$).

As expected, reserves are the largest for the S = 32 m, H = 6 m, Snow = 150 $kN/m^2$ frame. In this case the large span and large value of the vertical load makes the vertical ULS combination controlling the design.

## 4.2 Nonlinear analysis

In order to determine the load bearing capacity of the studied frames, non-linear analysis has been carried out by gradually increasing the load on the frames. Two scenarios were studied: (i) vertical loads distributed to each purlin location have been increased gradually, (ii) frames have been loaded with the vertical load corresponding to the earthquake combination ($P_{ULS-EQ}$) and, after that, concentrated horizontal loads in the corners of the frames have been gradually increased until failure of the frames. The first loading scenario is meant to determine the vertical capacity of the frames, while the second loading scenario is a classical pushover analysis.

Base material of the frames was steel S275, with $f_y$ = 275 $N/mm^2$, and fracture at $f_u$ = 430 $N/mm^2$ and ε = 0.06. Geometric nonlinearity was considered in the models.

Quite large imperfection amplitudes were taken into account. These imperfections were based on the previously determined first buckling shape (almost always LTB). As LTB was the presumed failure mode, imperfections were included only at member level, as initial bow. The amplitude of the imperfections were based on §5.3.4 of prEN1993-1-1 [1], and were taken as $e_0/L=0.5\times1/200$, where $e_0$ is the largest amplitude of the imperfection and L is the length of the element to which

the imperfection is applied. For simplicity, L was considered as half the span S in these calculations.

Hence, the out-of-plane amplitude of the imperfections was $a_2$ = 25 mm for 20 m span, $a_2$ = 40 mm for 32 m span and $a_2$ = 20 mm for 16 m span frames.

### 4.2.1 Behavior in case of vertical loading

The results of the analysis with vertical loading are presented in Figure 15. On the left side (Figure 15a, c, e, g) are presented the results for frames made of hot-rolled profiles; and on the right side (Figure 15b, d, f, h) for built-up welded frames. Curves on the right present the vertical distributed load (P) vs. the mid-span vertical displacement ($d_v$). The left curve presents the largest out of plane deformation ($d_{out}$). The uninterrupted blue line refers to the result with initial imperfection; while the dashed line refers to results without any imperfection. The red triangle marks the point where yielding in any fiber occurs in the model ($\sigma$ = 275 N/mm$^2$). The yellow diamond on the out-of plane deformation curve corresponds to the point where the tangent stiffness of the curve falls below 10% of the initial stiffness. It is considered that at that point in the loading history, lateral deformation is very large, and lateral buckling is inevitable. The minimum of the red triangle and yellow diamond corresponds to the load capacity of the frame.

The horizontal dotted black line corresponds to the vertical design load on the frame plus the mass of the frame transformed in distributed load: (1.35 × (1.4 × $M_{fr}$/(S × T)) × $P_{des}$). The mass was increased by 40% to take into account elements of the frame which have not been modeled in the FEM (e.g. plates) while 1.35 is the safety factor.

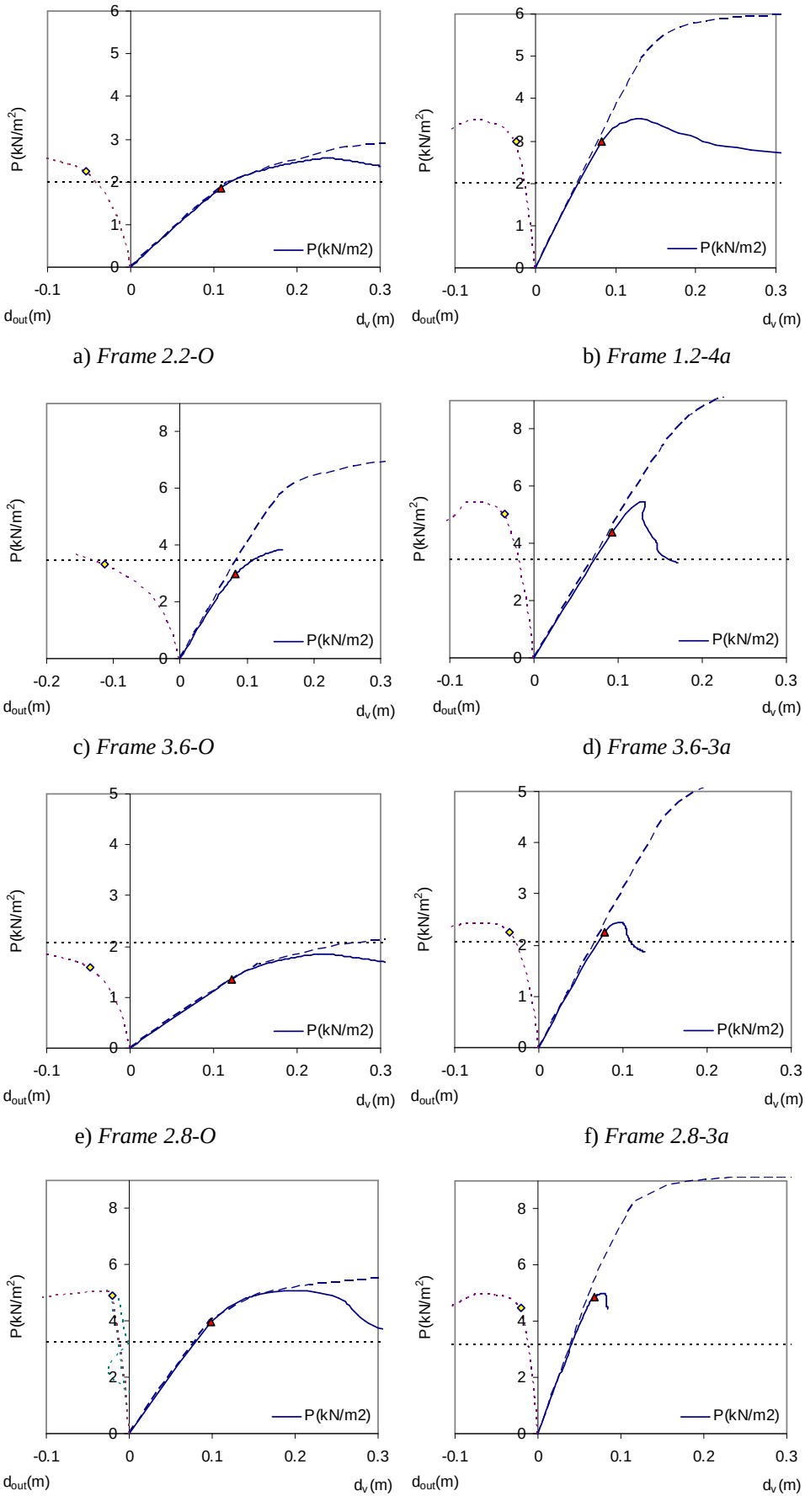


a) *Frame 2.2-O*

b) *Frame 1.2-4a*

c) *Frame 3.6-O*

d) *Frame 3.6-3a*

e) *Frame 2.8-O*

f) *Frame 2.8-3a*

g) *Frame 3.20-O*

h) *Frame 3.20-2a*

*Figure 15. Vertical load vs. mid-span deflection of the frames.*

A few observations concerning the results:

- It can be observed that only one (3.20-O) of the hot-rolled frames resists the vertical design loads. The situation is extremely bad in case of configuration 2.8-O, where the frame is short of the design load with 35%.
- The welded configurations are much more sensitive to imperfections than the hot-rolled ones. The exception is the 32 m span frame.
- Frame 3.20-O is not at all sensitive to imperfections.
- Welded tapered frames are stiffer than hot-rolled ones.

### 4.2.2 Behavior under horizontal loads

The results of the analysis with horizontal loads are presented in Figure 16. The pushover forces ($F_H$) have been transformed in spectral acceleration format considering the masses concentrated at the roof level ($M_{EQ}$). Curve types have the same meaning as for vertical loads: full blue line is pushover with imperfection of $a_2$ = 40 mm; dashed blue line is pushover without imperfection and red triangle is yield. The three elastic spectra in Figure 16 correspond to the elastic demand for $a_g$ = 0.08, 0.16 & 0.32 g (Type 1, Soil B spectra in EN1998). The elastic period of vibration has been evaluated and is presented in the figure by $T_e$.

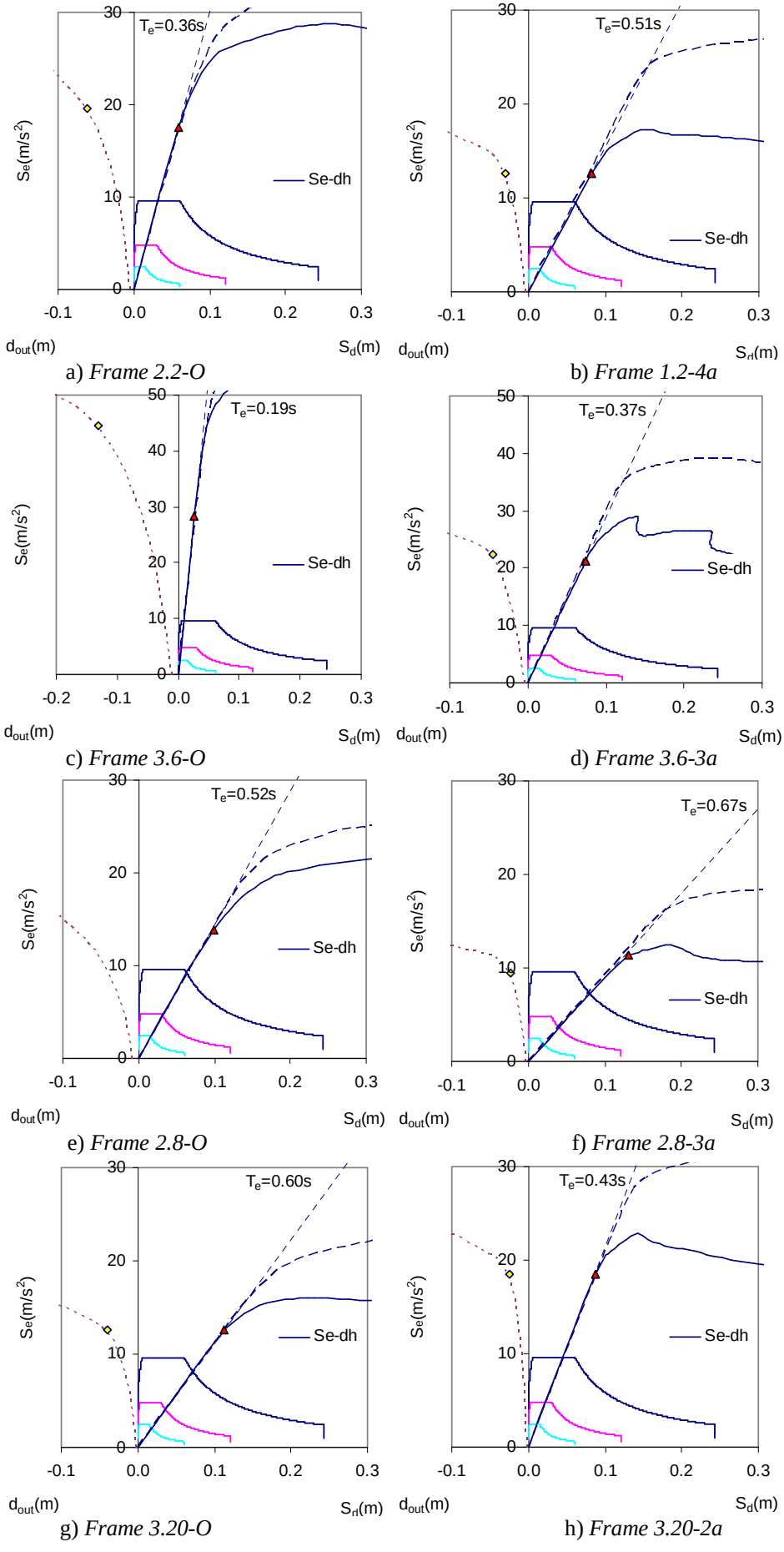


*Figure 16. Push-over curves of the frames vs. demand.*

The following can be observed based on the curves:

- In all cases the frames configured only from vertical loads satisfy the ULS requirements for earthquake even for the very high value of PGA = 0.32g. (NOTE: Results in Table 4 suggested that Frame 2.8-O would not be satisfactory.)
- Hot-rolled frames are stiffer because they are fixed at the base, while tapered frames are pinned (e.g. configurations 2.2, 3.6 & 2.8). In the case when the hot-rolled frame was pinned (Configurations 3.20), the welded frame is stiffer.
- Both types of frames are moderately sensitive to imperfections, there is considerable difference between the behavior with and without imperfections.

The deformed shape of frames during the analysis is presented in Appendix B, while a summary description of the failure modes is presented in Table 5.

*Table 5. Description of failure modes from non-linear analysis.*

| | Imp. (mm) | Stage | Horizontal | Vertical |
|---|---|---|---|---|
| 2.2-O | 25 | Y | - Formation of a plastic hinge at the base of the right side column. (App B-Nr.1a) | - Shear yielding of the panel zone of the column to beam connection. (App B-Nr.2a) |
| | | F | - Yielding and buckling of the hinges at the base of both columns. Followed by LTB of the beam. (App B-Nr.1b) | - Shear deformation of the panel zone of the column to beam connection followed by LTB of the beam. (App B-Nr.2b) |
| 1.2-4c | | Y | - First yielding appears at the end of the tapered region of the beam. (App B-Nr.3a) | - LTB of the beam (App B-Nr.3b) |
| | | F | - First yield on the flanges of the column simultaneously with the flanges of the beam (App. B-Nr.4a) | - LTB of the corner region of the frame (beam and column flange simultaneously) (App B-Nr.4b) |
| 3.6-O | | Y | - First yielding at one of the column bases (App B-Nr.5a) | - Localized yielding of the beam flange in the column connection region. (App B-Nr.6a) |
| | | F | - Gradual yielding of the plastic hinge at the base is closely followed by LTB of the same side beam. (App B-Nr.5b) | - Beam LTB with no involvement of the column. (App B-Nr.6b) |
| 3.6-3a | 40 | Y | - Yielding of the beam at the end of the taper (App B-Nr.7a) | - Simultaneous yielding of the column flange and beam flange in the tapered region. (App B-Nr.8a) |
| | | F | - LTB of the beam (App B-Nr.7b) | - LTB of the beam in the tapered region. The column corner is very moderately involved in the buckling. In the last stage the deformation is localized in two waves on the flanges of the tapered beam and the column. (App B-Nr.8b) |
| 2.8-O | | Y | - Yielding at the base of one column. (App B-Nr.9a) | - Shear yielding of the panel zone of the column to beam connection. (App B-Nr.10a) |
| | | F | - LTB of the beam. (App B-Nr.9b) | - LTB of the beams. (App B-Nr.10b) |
| 2.8-3a | 25 | Y | - Yielding of the beam flange at the end of the tapered portion. (App B-Nr.11a) | - Simultaneous yielding of both the column flange and beam flange in the tapered region. (App B-Nr.12a) |
| | | F | - LBT of the beam and the column flange simultaneously. Later the whole corner of the frame involved in the deformation. (App B-Nr.11b) | - LTB of the one column flange. (App B-Nr.12b) |
| 3.20-O | | Y | - Yielding of beam flange at the end of the haunch region. (App. B-Nr.13a) | - Shear failure of the web panel in the column-beam connection. (App B-Nr.14a) |
| | | F | - LTB of the beam. (App B-Nr.13b) | - Shear yielding of the web panel zone, followed by LTB of the beam in the haunch region. (App B-Nr.14b) |
| 3.20-2a | 20 | Y | - Yielding of the beam flange at the end of the taper. (App B-Nr.15a) | - Simultaneous yielding of the flange of the column and the flange of the beam in the tapered region. (App B-Nr.16a) |
| | | F | - LTB starting simultaneously at the flange of the beam in the tapered region and the flange of the column. Later the whole frame corner is involved in the deformation. (App B-Nr.15b) | - LTB of the column flange. (App B-Nr.16b) |

### 4.2.3 Relation between the linear & non-linear analysis results

The representative values, from both the vertical and horizontal non-linear analysis, are summarized in Table 6. It can be observed that most of the time the

criteria corresponding to yielding is governing that load capacity of the frame. Exceptions are Frame 28-3a under horizontal loads, and Frame 3.20-2a under vertical loads.

*Table 6. Summary of yield ($F_{Hy}$, $P_{Vy}$) and buckling ($F_{Hb}$, $P_{Vb}$) loads of the frames.*

| | Horizontal | | | | | Vertical | | | | |
|---|---|---|---|---|---|---|---|---|---|---|
| | $F_{Hy}$ (kN) | $d_{Hy}$ (m) | $F_{Hb}$ (kN) | $d_{Hb}$ (m) | Check | $P_{Vy}$ (kN/m$^2$) | $d_{Vy}$ (m) | $d_{Vb}$ (m) | $P_{Vb}$ (kN/m$^2$) | Check |
| 2.2-O | 134.3 | 0.059 | 150.2 | 0.067 | - | 1.85 | 0.109 | 0.154 | 2.25 | NO |
| 1.2-4c | 98.2 | 0.083 | 98.2 | 0.083 | - | 2.98 | 0.082 | 0.082 | 2.98 | - |
| 3.6-O | 486.1 | 0.026 | 766.2 | 0.048 | - | 2.97 | 0.083 | 0.100 | 3.34 | NO |
| 3.6-3a | 353.4 | 0.074 | 370.9 | 0.078 | - | 4.40 | 0.093 | 0.109 | 5.04 | - |
| 2.8-O | 115.9 | 0.099 | 161.4 | 0.170 | - | 1.36 | 0.122 | 0.150 | 1.60 | NO |
| 2.8-3a | 94.5 | 0.132 | 78.7 | 0.106 | - | 2.26 | 0.079 | 0.079 | 2.26 | - |
| 3.20-O | 87.1 | 0.113 | 87.1 | 0.113 | - | 3.68 | 0.088 | 0.136 | 4.75 | - |
| 3.20-2a | 117.5 | 0.088 | 117.5 | 0.088 | - | 4.87 | 0.068 | 0.059 | 4.46 | - |

As discussed earlier, a linear-elastic design check of the frames should be carried out according to Eq. (1). This expression, has been used to determine the values of the vertical load that can be resisted by the frame $P_{DIST}$, presuming that the reduction factor $\chi_{OP}$ corresponding to the frame slenderness $\lambda_{OP}$ is known. In fact, the relationship between the two was supposed according to the buckling Curve B [1] for hot rolled frames, and buckling Curve D [1] for welded frames.

$$\frac{\chi_{OP} \cdot \alpha_{ult,k}}{\gamma_{M1}} \leq 1 \Rightarrow P_{DIST} \leq \frac{\chi_{OP}}{\gamma_{M1}} \cdot P_{yield}, \quad \text{and} \quad \chi_{OP} = f(\lambda_{OP}) \tag{7}$$

In the above expression $P_{yield}$ is the load corresponding to the yielding of the most stressed fiber, if out of plane buckling is completely disregarded. If the safety factor is eliminated and the inequality is changed in equality, this means that the relationship $P_{DIST} = \chi_{OP} \cdot P_{yield}$ links the "yield load" to capacity of the frame. As the capacity of the frames have been calculated with the non-linear method $P_{DIST-NL} = \min(P_{Vy}, P_{Vb})$, the reduction factors corresponding to these loads ($\chi_{OP\_NL}$) can be deduced as: $\chi_{OP\_NL} = \frac{P_{yield}}{P_{DIST\_NL}}$. The values of the slenderness of the frames ($\lambda_{OP}$), the value of the old theoretical/code reduction factor ($\chi_{OP}$) and the reduction factor from the non-linear analysis ($\chi_{OP\_NL}$) are presented in Table 7 and Figure 17.

*Table 7. Slenderness and reduction factor for frames.*

| | $\lambda_{OP}$ | $\chi_{OP}$ | $P_{yield}$ (kN/m$^2$) | $P_{DIST}$ (kN/m$^2$) | $P_{DIST\_NL}$ (kN/m$^2$) | $\chi_{OP\_NL}$ |
|---|---|---|---|---|---|---|
| 22-O | 0.86 | 0.69 | 1.99 | 1.24 | 1.85 | 0.93 |
| 12-4a | 0.93 | 0.51 | 4.04 | 1.86 | 2.98 | 0.74 |
| 3.6-O | 0.99 | 0.60 | 3.57 | 1.96 | 2.97 | 0.83 |
| 3.6-3a | 0.77 | 0.60 | 5.33 | 2.91 | 4.40 | 0.83 |
| 2.8-O | 0.86 | 0.68 | 2.01 | 1.25 | 1.36 | 0.68 |
| 2.8-3a | 1.11 | 0.42 | 4.82 | 1.82 | 2.26 | 0.47 |
| 3.20-O | 0.70 | 0.78 | 3.91 | 2.78 | 3.68 | 0.94 |
| 3.20-2a | 0.93 | 0.50 | 6.06 | 2.76 | 4.46 | 0.74 |

From Figure 17 it is evident that:

- The slenderness values of the hot-rolled and welded frames are comparable. One might expect that hot-rolled frames are less slender because of the compactness of the cross-sections, but when it comes to lateral torsional buckling, it seems, that the advantage of compactness less relevant.
- Both hot-rolled and welded frames seam to have less capacity reduction ($\chi_{OP}$) due to buckling than suggested by the curves used in the design. One notable exception is Frame 2.8-O. Welded frames are more sensitive to buckling than rolled ones, but in both cases the use of higher buckling curves seems possible (e.g. Curve B, using Eq.6.57 from prEN1993-1-1, with parameters $\beta = 1.5$ and $\lambda_{LT,0} = 0.4$ is comparatively presented in Figure 17). One important weakness of the non-linear analysis performed here is, that residual stresses were not included in the study. Welded sections are more prone to residual stresses than rolled ones, and in both cases, residual stresses can have important influence on the non-linear curves. Therefore, the suggestion of using different buckling curves could only be made based on a more thorough investigation, not on the few result obtained here. However, it is believed that the important gain of load bearing capacity that could be demonstrated calls for such future studies.

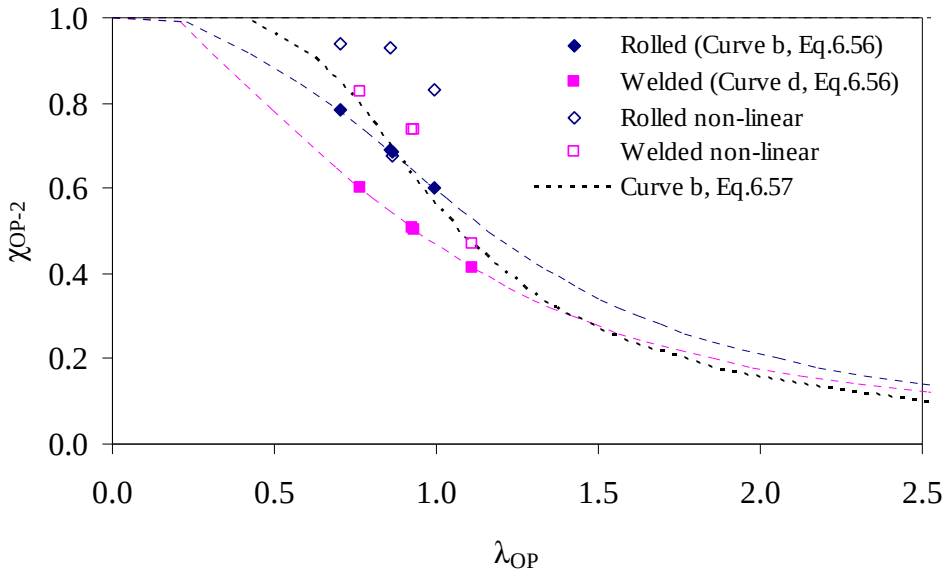


*Figure 17. Comparative plot of theoretical reduction factor ($\chi_{OP}$) and the one obtained by non-linear analysis ($\chi_{OP\_NL}$).*

## 4.3 LGS - light-gauge steel frames

In the study it has been attempted to use LGS elements for the manufacturing of the frame. Particularly, the use of the two back-to back C shaped profiles as beams and columns have been investigated using the non-linear modeling procedure previously described.

The LGS beams were supposed to be connected by welded corner pieces. These pieces were configured so that they do not fail during loading. (Figure 18).

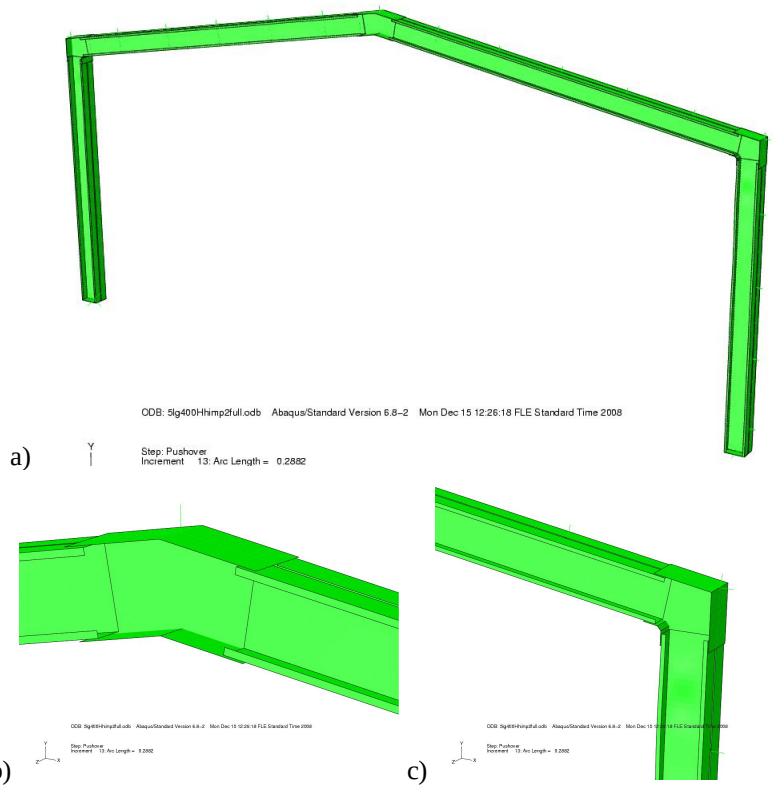


*Figure 18. Configuration of LGS frame with back-to-back C elements and corner fixings.*

From among the geometries studied in the previous chapters, the cases of 16 m and 20 m span frames were tried. The base of the frames has been chosen as fixed or hinged, depending on the observed requirements. Both 0.75 kN/m$^2$ and 1.5 kN/m$^2$ has been considered. The cold-formed profile catalog of the company KONTI [10] has been used as basis for the choosing the shapes of the LGS profiles. The initial shapes of the LGS profiles (Figure 19a) have been simplified to a simple C (Figure 19b) but maintaining the overall dimensions. This was necessary in order to avoid overcomplicating the FE model. The eliminated features are stiffening the profile, and therefore they are beneficial. It is presumed that by eliminating these features, the load bearing capacity of the frames is lowered in every load combination. The yield stress was considered $f_y$ = 350 N/mm$^2$, a typical value for most LGS steel profiles.

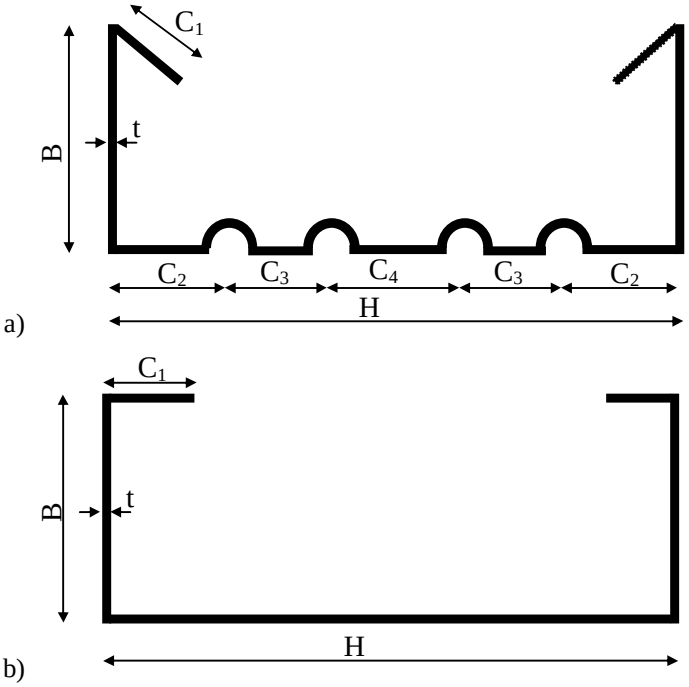


*Figure 19. Initial KONTI profile (a) and simplified shape use din the analysis (b).*

*Table 8. Shape parameters of the KONTI profiles considered.*

| | H (mm) | B (mm) | $C_1$ (mm) | $C_2$ (mm) | $C_3$ (mm) | $C_4$ (mm) | t (mm) |
|---|---|---|---|---|---|---|---|
| KO 350×3 | 350 | 79.5 | 35 | 120 | 110 | 0 | 3 |
| KO 400×3.5 | 400 | 80 | 35 | 120 | 160 | 0 | 3.5 |
| KO 450×4 | 450 | 80.5 | 35 | 120 | 210 | 0 | 4 |
| KO 500×5 | 500 | 81.5 | 35 | 120 | 85 | 90 | 5 |
| KO 550×5 | 550 | 81.5 | 35 | 120 | 110 | 90 | 5 |
| KO 600×5 | 600 | 81.5 | 35 | 120 | 135 | 90 | 5 |

In the case of the LGS frames, the analysis using the method from Chapter 4.1 is impossible to apply. The thin profiles of the LGS frame always undergo local buckling at a fairly low level of load. However, this does not mean the failure of the frame, as the locally buckled thin profiles are capable of carrying larger load. Therefore, the first elastic buckling modes are local modes and they are not relevant in determining $\alpha_{cr,OP}$ needed for that analysis.

Having the impossibility to apply the simplified analysis method, full non-linear analysis of the frames was carried out according to the method presented in Chapter 4.2. The initial imperfections for the LGS frames were based on a combination of the first 20 buckling modes (i.e. all local and in different locations on the elements) with a presumed amplitude of the 2 mm. Because of the thinness of the profiles, it was impossible to obtain global buckling modes of the frames. However, it is believed that the inclusion of global buckling mode shapes is not crucial; the failure of the LGS frame, with this degree of lateral support, will be by local buckling degenerating into localized plastic mechanism. This failure mode has been observed on both component tests [12] and full scale frame test [13]. Global buckling of an element can cause the failure only if large lengths of the members are unsupported.

Resulting pushover curves are presented in Figure 20, and characteristic values are summarized in Table 3. The deformed shape and the corresponding stress states are presented in more detail in Appendix C.

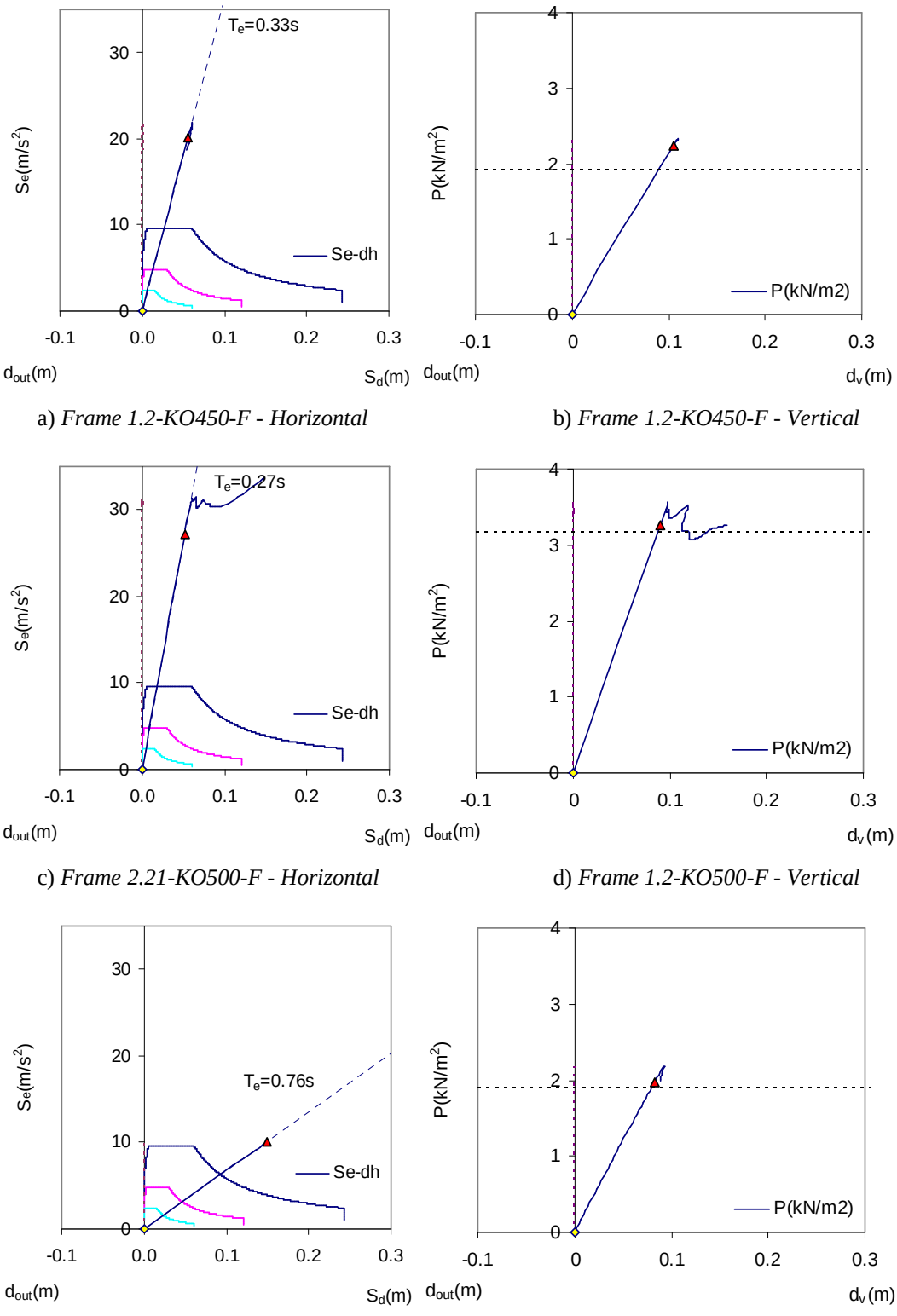


a) *Frame 1.2-KO450-F - Horizontal*

b) *Frame 1.2-KO450-F - Vertical*

c) *Frame 2.21-KO500-F - Horizontal*

d) *Frame 1.2-KO500-F - Vertical*

e) *Frame 1.1-KO400-P - Horizontal*

f) *Frame 1.1-KO400-P - Vertical*

*Figure 20. Pushover curves of the LGS frames.*

*Table 9. Design alternatives for detailed design of frames.*

| | Base | fy (N/mm$^2$) | S (m) | T (m) | $P_{des}$ (kN/m$^2$) | $h_c$ (mm) | $h_h$ (mm) | $h_b$ (mm) | b (mm) | $t_f$ (mm) | $t_w$ (mm) | Torsional restraint | $d_{Vy}$ (m) | $F_{Hy}$ (kN) | $d_{Hy}$ (m) | $P_{Vy}$ (kN/m$^2$) | $M_{fr}$ (kg) |
|---|---|---|---|---|---|---|---|---|---|---|---|---|---|---|---|---|---|
| 2.2-O | F | 275 | | | | | HEA300, IPE330 | | | | | - | 0.059 | 134.3 | 0.109 | 1.85 | 2215 |
| 1.2-4c | P | 275 | 20 | 6 | 1.64 | 200 | 800 | 400 | 260 | 10 | 8 | | 0.083 | 98.2 | 0.082 | 2.98 | 2291 |
| 2.2-450-F | F | 350 | | | | | 2×KO450×4 | | | | | - | 0.055 | 139.4 | 0.105 | 2.24 | 1704 |
| 2.21-500-F | F | 350 | 20 | 6 | 2.76 | | 2×KO500×5 | | | | | | 0.052 | 219.6 | 0.090 | 3.26 | 2500 |
| 1.1-400-P | P | 350 | 16 | 6 | 1.64 | | 2×KO400×3.5 | | | | | | 0.141 | 52.0 | 0.082 | 1.97 | 1300 |

The following preliminary conclusions can be drawn from these analysis cases:

- In the range of spans of 16 - 20 m the use of LGS frames is at least possible. The competitively of this frames depends very much on the requirements of the exact application and the comparative prices of the LGS steel and other steel products.
- It can be observed in Figure 20 that LGS frames posses no ductility. The linear loading stage is immediately followed by decrease of the capacity. This is expected in case of Class 4 elements undergoing bending.
- As previously, frames configured for vertical loads only are capable to resist the horizontal loads arising from earthquake in the elastic range. Therefore, the design of these frames is not controlled by earthquake loads.
- One major question which has not been addressed by these models is the performance of the connection between the corner elements and the LGS steel profiles. Because of the difficulty to weld LGS these connections will have to bolted which can have an inherent weakness due to the thinness of the connected profiles (i.e. bearing failure of the bolted connection).
- If the frames are pinned at the base, they are more flexible than the welded-tapered configuration and they might be sensitive to horizontal displacement in the earthquake combination. Fixing the base of the frame is one solution. This will usually not increase significantly the capacity of the frame, but it will improve lateral stiffness. Base fixing has been used in case of 2.2-450-F and 2.21-500-F here, while 1.1-400-P is pinned. Therefore 1.1-400-P is very flexible (Figure 20e).

# 5 Conclusions

A significant number of frame geometries have been analyzed with different structural configurations. Three configurations were considered: (1) hot-rolled members with haunch, (2) tapered welded members and (3) LGS profiles with corner fixings. The following general conclusions can be drawn from the results:

- Both hot-rolled and welded frames are sensitive to LTB. The frame slenderness is in the range of $\lambda_{OP}$ = 1 for welded frames, $\lambda_{OP}$ = 0.6 - 0.8 for welded frames with LTB support and $\lambda_{OP}$ = 0.8 for hot rolled frames (Figure 21). Besides the type of the frame, it is clear from Figure 21 that slenderness depends on the

geometrical configuration (e.g. span). This slenderness has an important effect on the design, which seems not to always have been properly taken into account by the pre-design methodology of the PRECASTEEL project [3]; as almost all hot-rolled frames were slightly underdesigned (Obs. at least from the point of view of the method from Chapter 4.1, corresponding to prEN 1993-1-1).

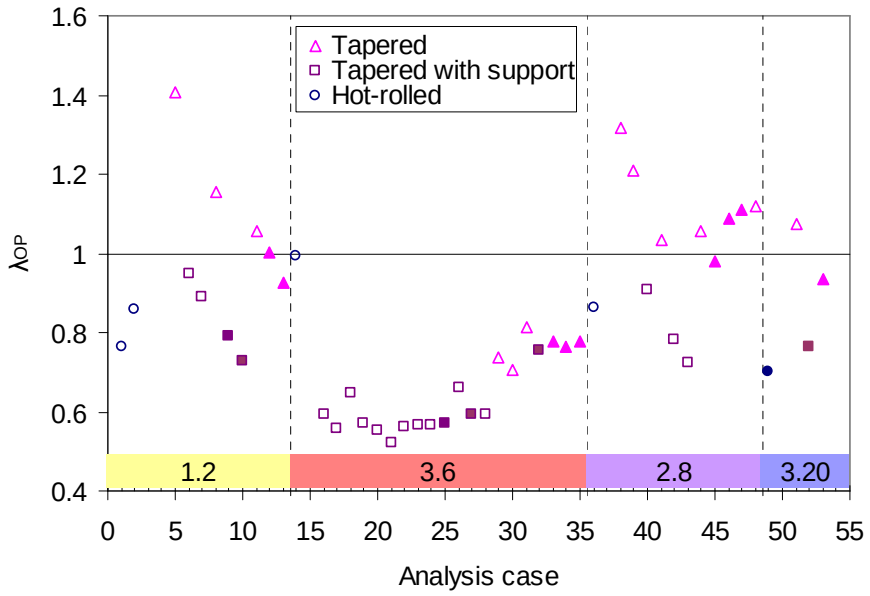


*Figure 21. Slenderness of analyzed frames, full symbols correspond to frames satisfying design requirements.*

- It appears from the non-linear analysis (Chapter 4.2) that the frames are less sensitive to LTB than predicted by the elastic design of Chapter 4.1; even if the failure mode observed during non-linear analysis was also LTB. Larger design load was obtained from the non-linear analysis, compared to the elastic analysis, suggesting that a higher buckling curve could be used in the elastic design, than the ones used in Chapter 4.1 (see Figure 17).
- Tapered-welded frames were more economical on for the same geometry than hot-rolled frames. This conclusion is made from the point of view of steel consumption (Table 3), and is true even in the case when torsional support was not used to avoid LTB. Tapered-welded frames are hinged at the base, giving additional advantage compared to fixed-base hot-rolled frames (i.e. smaller foundations needed). However, the overall economicity of the two solutions must be assessed by comparing these advantages with the increased labor cost of the welded frames.
- Torsional supports preventing the LTB of the frames are very effective in decreasing slenderness and reducing steel consumption. However, it should be noted that these supports are not always as effective as often believed (Table 1). If torsion supports are utilized in the design, then the designer should make sure that the provided support is adequate both as strength but also as stiffness.
- Distributed torsional support can be as effective as concentrated support (e.g. proving small torsion stiffness at each purlin vs. torsion blocking at the corner of the frame). Minor details are sometimes very important.
- For all frames, the primary design criterion was ULS from vertical loads. The ULS from earthquake loads (PGA = 0.32 g) was satisfied, in the elastic range of

response, by the frames configured for vertical loads. The simplified, Chapter 4.1, analysis was predicting that configurations 1.2-4a and 2.8-3a would fail in the ULS horizontal load check (Table 4). Non-linear analysis was predicting much larger capacity both for vertical and horizontal loads, than the simplified analysis.

- LGS frames are satisfactory for vertical load ULS up to spans of 16 - 20 m, even with the higher snow loads values of 1.50 kN/m$^2$. In the earthquake ULS these frames resist the horizontal load entirely by elastic response (Figure 20). Not surprisingly, since they are made of Class 4 profiles, these frames have no ductility at all, but their elastic capacity is a few times larger than the demand at PGA = 0.32 g. Therefore, their safety in earthquake is ensured by their elastic capacity.

## References

[1] prEN1993-1-1, Eurocode 3: Design of steel structures - Part 1-1: General rules and rules for buildings.

[2] Holicky, M.; Sykora, M. Models for exposure conditions - A review of available data for snow and flooding in the Czech Republic; ETH Zurich: Zurich, 2008; (*Presentation Slide*)

[3] Varelis, G.; Vasilikis, D.; Karamanos, S.; Tsintzos P. Preliminary design for industrial buildings; University of Thessaly: 2008.

[4] prEN1990 Eurocode - Basis of structural design; European Committee for Standardization: Busseles, 2001.

[5] http://www.lindabprofile.com/frameset/run_frameL3.asp?LangRef=20&Area=15&topID=3&ArticleID=9965&MenuID=174&Template=../templates/a_masterweb_standard.asp&ExpandID=2329&T=39&P=9132.

[6] prEN1993-1-3, Eurocode 3: Design of steel structures - Part 1-3: General rules - Supplementary rules for cold-formed members and sheeting.

[7] EN1998: Design of structures for earthquake resistance, Part 1: General rules, seismic actions and rules for buildings.

[8] Zaharia R., Dubina D., Stiffness of joints in bolted connected cold-formed steel trusses, Journal of constructional steel research, 62(2006) 240-249.

[9] Dubina D., Zaharia R., Cold-formed steel trusses with semi-rigid joints, Thin-Walled Structures Vol. 29, Nos. 1-4, pp. 273 - 287, 1997.

[10] http://www.kontirom.ro/produse/profile_cu_pereti_subtiri/profile_kb.htm

[11] Paul Beaucaire, Performance analysis of selected steel types for one-storey industrial buildings solutions, VTT-R-00133-09.

[12] Nagy, Zs.; Stratan, A.; Dubina, D. Application of component method for bolted cold-formed steel joints; Taylor & Francis: Poiana Brasov, Romania, 2006;

[13] Nagy, Zs. Studiul Solutiilor Constructive si Performantelor Structurale ale Halelor Usoare cu Structura Realizata din Profile de Otel Formate la Rece (eng. Detailing and Structural Performance of hall with Structure made of LGS); University Politehnica of Timisoara: Timisoara, 2006;

*Appendix A. Summary of results for analyzed frame configurations.*

| Nr. | Name | S (m) | T (m) | $P_{des}$ (kN/m$^2$) | $h_c$ (mm) | $h_h$ (mm) | $h_b$ (mm) | b (mm) | $t_f$ (mm) | $t_w$ (mm) | Torsional restraint | $\lambda_{OP}$ | $\chi_{OP-1}$ | $\alpha_{cr,OP}$ | $\alpha_{ult,k}$ | $\sigma_{max}$ (N/mm$^2$) | $P_{yield}$ (kN/m$^2$) | $P_{DIST}$ (kN/m$^2$) | M (kg) | $P_M$ (kN/m$^2$) | $P_{ULS}$ (kN/m$^2$) | Web c/t= 91.89 | Flange c/t= 12.94 | Notes |
|---|---|---|---|---|---|---|---|---|---|---|---|---|---|---|---|---|---|---|---|---|---|---|---|---|
| **Case 1.2, Load = 1.64 kN/m$^2$** | | | | | | | | | | | | | | | | | | | | | | | | |
| 1 | 1.2-O | | | | | | HEA300, IPE360 | | | | - | 0.76 | 0.75 | 2.22 | 1.29 | 213 | 2.12 | 1.44 | 2412 | 0.20 | 1.24 | | | |
| 2 | 2.2-O | | | | | | HEA300, IPE330 | | | | - | 0.86 | 0.69 | 1.65 | 1.21 | 227 | 1.99 | 1.24 | 2215 | 0.18 | 1.06 | | | |
| 3 | 1.2-O+ | | | | | | HEA300, IPE360 | | | | - | 0.73 | 0.77 | 2.43 | 1.29 | 213 | 2.12 | 1.48 | 2412 | 0.20 | 1.28 | | | PUF |
| 4 | 2.2-O+ | | | | | | HEA300, IPE330 | | | | - | 0.81 | 0.72 | 1.85 | 1.21 | 227 | 1.99 | 1.30 | 2215 | 0.18 | 1.11 | | | PUF |
| 5 | | a | | | 200 | 800 | 400 | 180 | 8 | 8 | - | 1.41 | 0.30 | 0.83 | 1.65 | 166 | 2.71 | 0.75 | 1689 | 0.14 | 0.61 | Cl4 | Ok | |
| 6 | 1.2-1 | b | | | 200 | 800 | 400 | 180 | 8 | 8 | C | 0.95 | 0.49 | 1.84 | 1.65 | 166 | 2.71 | 1.22 | 1689 | 0.14 | 1.08 | Cl4 | Ok | |
| 7 | | c | 20 | 6 | 1.64 | 200 | 800 | 400 | 180 | 8 | 8 | C+T | 0.89 | 0.53 | 2.09 | 1.65 | 166 | 2.71 | 1.30 | 1689 | 0.14 | 1.16 | Cl4 | Ok | |
| 8 | | a | | | | 200 | 800 | 400 | 220 | 8 | 8 | - | 1.15 | 0.39 | 1.43 | 1.90 | 144 | 3.12 | 1.12 | **1855** | 0.15 | 0.97 | Cl4 | Ok | |
| 9 | 1.2-2 | b | | | | 200 | 800 | 400 | 220 | 8 | 8 | C | 0.79 | 0.59 | 3.05 | 1.90 | 144 | 3.12 | 1.66 | 1855 | 0.15 | 1.51 | Cl4 | Ok | |
| 10 | | c | | | | 200 | 800 | 400 | 220 | 8 | 8 | C+T | 0.73 | 0.62 | 3.59 | 1.90 | 144 | 3.12 | 1.77 | 1855 | 0.15 | 1.62 | Cl4 | Ok | 0.23 |
| 11 | 1.2-3 | a | | | | 200 | 800 | 400 | 240 | 8 | 8 | - | 1.06 | 0.44 | 1.81 | 2.03 | 135 | 3.33 | 1.33 | 1938 | 0.16 | 1.17 | Cl4 | Cl4 | |
| 12 | | b | | | | 200 | 800 | 400 | 240 | 10 | 8 | - | 1.00 | 0.47 | 2.30 | 2.31 | 119 | 3.79 | 1.61 | 2187 | 0.18 | 1.42 | Cl4 | Ok | |
| 13 | 1.2-4 | a | | | | 200 | 800 | 400 | 260 | 10 | 8 | - | 0.93 | 0.51 | 2.87 | 2.46 | 112 | 4.04 | 1.86 | **2291** | 0.19 | 1.67 | Cl4 | Ok | 0.05 |
| **Case 3.6: Load: = 2.76 kN/m$^2$** | | | | | | | | | | | | | | | | | | | | | | | | |
| 14 | 3.6-O | | | | | | HEA650, IPE600 | | | | - | 0.99 | 0.60 | 1.32 | 1.29 | 213 | 3.57 | 1.96 | 7051 | 0.37 | 1.59 | | | |
| 15 | 3.6-O+ | | | | | | HEA650, IPE600 | | | | | 0.93 | 0.64 | 1.49 | 1.29 | 213 | 3.57 | 2.08 | 7051 | 0.37 | 1.71 | | | PUF |
| 16 | 3.6-10 | | | | 250 | 1000 | 500 | 320 | 12 | 10 | C+T+M | 0.59 | 0.72 | 2.70 | 0.94 | 291 | 2.60 | 1.69 | 4754 | 0.25 | 1.45 | Cl4 | Ok | LB |
| 17 | 3.6-11 | | | | 225 | 900 | 450 | 320 | 12 | 10 | C+T+M | 0.56 | 0.74 | 2.63 | 0.82 | 337 | 2.25 | 1.52 | 4549 | 0.24 | 1.28 | Ok | Ok | LB |
| 18 | 3.6-12 | | | | 300 | 1200 | 600 | 320 | 14 | 10 | C+T | 0.65 | 0.68 | 3.14 | 1.32 | 208 | 3.66 | 2.25 | 5620 | 0.29 | 1.96 | Cl4 | Ok | LB |
| 19 | 3.6-13 | | | | 240 | 960 | 480 | 380 | 14 | 10 | C+T | 0.57 | 0.73 | 3.41 | 1.11 | 248 | 3.07 | 2.03 | 5725 | 0.30 | 1.74 | Cl4 | Ok | LB |
| 20 | 3.6-14 | | 32 | 6 | 2.76 | 225 | 900 | 400 | 380 | 14 | 10 | C+T | 0.55 | 0.74 | 3.27 | 1.01 | 273 | 2.78 | 1.87 | 5495 | 0.29 | 1.59 | Ok | Ok | |
| 21 | 3.6-15 | | | | | 225 | 900 | 400 | 380 | 14 | 12 | C+T | 0.52 | 0.77 | 3.90 | 1.05 | 261 | 2.90 | 2.02 | 5840 | 0.30 | 1.72 | Ok | Ok | |
| 22 | 3.6-16 | | | | | 275 | 1100 | 500 | 380 | 14 | 12 | C+T | 0.56 | 0.74 | 4.40 | 1.38 | 199 | 3.82 | 2.56 | 6335 | 0.33 | 2.23 | Ok | Ok | |
| 23 | 3.6-1 | a | | | | 300 | 1200 | 600 | 300 | 14 | 12 | C+T | 0.57 | 0.73 | 4.19 | 1.34 | 205 | 3.70 | 2.47 | 5901 | 0.31 | 2.16 | Cl4 | Ok | 0.16 |
| 24 | | b | | | | 300 | 1200 | 600 | 300 | 14&12 | 12&10 | C+T | 0.57 | 0.73 | 4.13 | 1.32 | 208 | 3.65 | 2.43 | 5515 | 0.29 | 2.14 | | | 0.22 |
| 25 | 3.6-17 | | | | | 300 | 1200 | 600 | 320 | 14 | 12 | C+T | 0.57 | 0.73 | 4.29 | 1.40 | 197 | 3.86 | 2.56 | 6102 | 0.32 | 2.24 | Cl4 | Ok | |

| | | | | | | | | | | | | | | | | | | | | | | | | |
|---|---|---|---|---|---|---|---|---|---|---|---|---|---|---|---|---|---|---|---|---|---|---|---|---|
| 26 | 3.6-18 | | | | 300 | 1200 | 500 | 380 | 14 | 10 | C+T | 0.66 | 0.67 | 3.39 | 1.48 | 185 | 4.10 | 2.49 | 6015 | 0.31 | 2.18 | Cl4 | Ok | |
| 27 | 3.6-4 | a | | | 300 | 1200 | 500 | 380 | 14 | 12 | C | 0.59 | 0.71 | 4.41 | 1.56 | 176 | 4.30 | 2.79 | 6458 | 0.34 | 2.46 | Cl4 | Ok | 0.08 |
| 28 | | b | | | 300 | 1200 | 500 | 380 | 14 | 12 | C+T | 0.59 | 0.71 | 4.42 | 1.56 | 176 | 4.30 | 2.79 | **6458** | 0.34 | 2.46 | Cl4 | Ok | 0.08 |
| 29 | 3.6-19 | | | | 300 | 1200 | 600 | 380 | 14 | 10 | - | 0.74 | 0.62 | 2.75 | 1.50 | 183 | 4.14 | 2.33 | 6222 | 0.32 | 2.00 | Cl4 | Ok | |
| 30 | 3.6-20 | | | | 300 | 1200 | 600 | 400 | 14 | 10 | - | 0.71 | 0.64 | 3.12 | 1.56 | 176 | 4.30 | 2.50 | 6423 | 0.33 | 2.17 | Cl4 | Cl4 | |
| 31 | 3.6-2 | a | | | 350 | 1400 | 600 | 360 | 14 | 10 | - | 0.82 | 0.57 | 2.69 | 1.79 | 154 | 4.94 | 2.56 | 6225 | 0.32 | 2.24 | Cl4 | Ok | |
| 32 | | | | | 350 | 1400 | 600 | 360 | 14 | 10 | C | 0.75 | 0.61 | 3.14 | 1.79 | 154 | 4.94 | 2.73 | 6225 | 0.32 | 2.41 | Cl4 | Ok | LB |
| 33 | 3.6-21 | | | | 350 | 1400 | 600 | 380 | 14 | 10 | - | 0.78 | 0.59 | 3.07 | 1.86 | 148 | 5.13 | 2.77 | 6426 | 0.33 | 2.43 | Cl4 | Ok | |
| 34 | 3.6-3 | a | | | 350 | 1400 | 600 | 400 | 14 | 10 | - | 0.77 | 0.60 | 3.29 | 1.93 | 142 | 5.33 | 2.91 | **6628** | 0.35 | 2.57 | Cl4 | Cl4 | 0.06 |
| 35 | 3.6-5 | a | | | 350 | 1400 | 600 | 380 | 14 | 12 | - | 0.78 | 0.59 | 3.22 | 1.96 | 140 | 5.40 | 2.91 | 6947 | 0.36 | 2.55 | Cl4 | Ok | 0.01 |
| | | | | | | | | | | | **Case 2.8: Load = 1.64 kN/m$^2$** | | | | | | | | | | | | | |
| 36 | 2.8-O | | | | | | HEA320, IPE330 | | | | - | 0.86 | 0.68 | 1.64 | 1.23 | 224 | 2.01 | 1.25 | 2711 | 0.23 | 1.03 | | | |
| 37 | 2.8-O+ | | | | | | HEA320, IPE330 | | | | - | 0.82 | 0.71 | 1.82 | 1.23 | 224 | 2.01 | 1.30 | 2711 | 0.23 | 1.08 | | | PUF |
| 38 | 2.8-10 | | | | 200 | 800 | 400 | 220 | 8 | 8 | - | 1.32 | 0.33 | 1.07 | 1.85 | 148 | 3.04 | 0.92 | 2089 | 0.17 | 0.75 | Cl4 | Ok | |
| 39 | 2.8-11 | | | | 150 | 600 | 300 | 220 | 8 | 8 | - | 1.21 | 0.37 | 0.87 | 1.27 | 217 | 2.08 | 0.70 | 1821 | 0.15 | 0.55 | Ok | Ok | |
| 40 | | | | | 150 | 600 | 300 | 220 | 8 | 8 | C+T | 0.91 | 0.52 | 1.54 | 1.27 | 217 | 2.08 | 0.98 | 1821 | 0.15 | 0.82 | Ok | Ok | |
| 41 | 2.8-12 | | | | 150 | 600 | 300 | 260 | 8 | 8 | - | 1.03 | 0.45 | 1.35 | 1.45 | 190 | 2.38 | 0.97 | 2005 | 0.17 | 0.81 | Ok | Cl4 | |
| 42 | | 20 | 6 | 1.64 | 150 | 600 | 300 | 260 | 8 | 8 | C+T | 0.78 | 0.59 | 2.37 | 1.45 | 190 | 2.38 | 1.28 | 2005 | 0.17 | 1.11 | Ok | Cl4 | |
| 43 | 2.8-13 | | | | 125 | 500 | 300 | 280 | 8 | 8 | C+T | 0.72 | 0.63 | 2.46 | 1.29 | 213 | 2.12 | 1.21 | 2013 | 0.17 | 1.04 | Ok | Cl4 | |
| 44 | 2.8-1 | a | | | 200 | 800 | 400 | 260 | 10 | 8 | - | 1.06 | 0.44 | 2.15 | 2.40 | 115 | 3.93 | 1.57 | 2577 | 0.21 | 1.36 | Cl4 | Ok | |
| 45 | 2.8-14 | | | | 150 | 600 | 400 | 260 | 10 | 8 | - | 0.98 | 0.48 | 1.91 | 1.83 | 150 | 3.01 | 1.30 | 2410 | 0.20 | 1.10 | Ok | Ok | |
| 46 | 2.8-15 | | | | 225 | 900 | 400 | 260 | 10 | 8 | - | 1.09 | 0.42 | 2.30 | 2.73 | 101 | 4.47 | 1.72 | 2661 | 0.22 | 1.50 | Cl4 | Ok | |
| 47 | 2.8-3 | a | | | 240 | 960 | 400 | 260 | 10 | 8 | - | 1.11 | 0.42 | 2.40 | 2.94 | 93 | 4.82 | 1.82 | **2711** | 0.23 | 1.60 | Cl4 | Ok | 0.00 |
| 48 | 2.8-16 | | | | 250 | 1000 | 400 | 260 | 10 | 8 | - | 1.12 | 0.41 | 2.46 | 3.09 | 89 | 5.06 | 1.89 | 2745 | 0.23 | 1.66 | Cl4 | Ok | |
| | | | | | | | | | | | **Case 3.20: Load: = 2.76 kN/m$^2$** | | | | | | | | | | | | | |
| 49 | 3.20-O | | | | | | HEA340, IPE360 | | | | - | 0.70 | 0.78 | 2.87 | 1.42 | 194 | 3.91 | 2.78 | 2355 | 0.25 | 2.53 | | | Hinged |
| 50 | 3.20-O+ | | | | | | HEA340, IPE360 | | | | - | 0.67 | 0.80 | 3.17 | 1.42 | 194 | 3.91 | 2.85 | 2355 | 0.25 | 2.60 | | | Hinged PUF |
| 51 | 3.20-1 | a | 16 | 6 | 2.76 | 200 | 800 | 400 | 220 | 8 | 8 | - | 1.08 | 0.43 | 1.56 | 1.81 | 152 | 4.99 | 1.95 | 1625 | 0.17 | 1.78 | Cl4 | Ok | |
| 52 | | b | | | | 200 | 800 | 400 | 220 | 8 | 8 | C | 0.76 | 0.60 | 3.10 | 1.81 | 152 | 4.99 | 2.73 | **1625** | 0.17 | 2.56 | Cl4 | Ok | 0.31 |
| 53 | 3.20-2 | a | | | | 200 | 800 | 400 | 240 | 10 | 8 | - | 0.93 | 0.50 | 2.52 | 2.19 | 125 | 6.06 | 2.76 | **1917** | 0.20 | 2.56 | Cl4 | Ok | 0.19 |

PUF - Purlins fixed at the level of the upper flange
LB - Failure by local buckling

*Appendix B. Stress state at yield and deformed shape at the ultimate state (largest displacement converged in ABAQUS).*

| | Nr. | | Yield (Von Mises stress) | Ultimate (Displacement amplitude) |
|---|---|---|---|---|
| | | | (a) | (b) |
| 1.2-O | 1 | Horizontal | 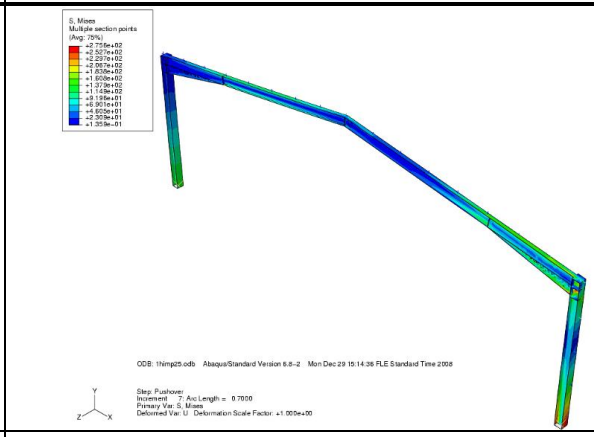 | 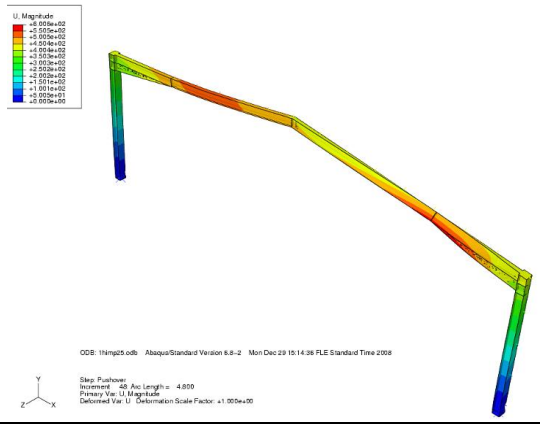 |
| | 2 | Vertical | 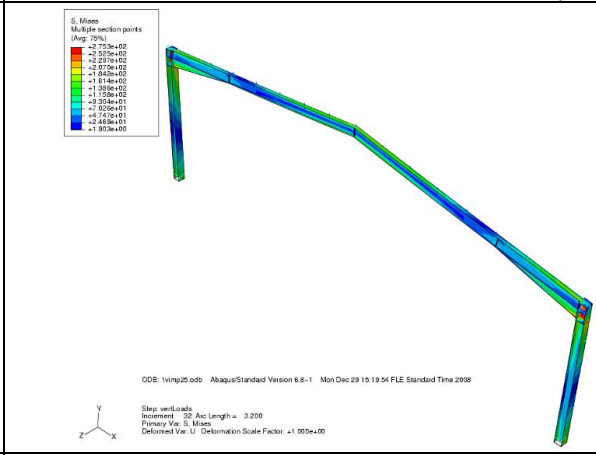 | 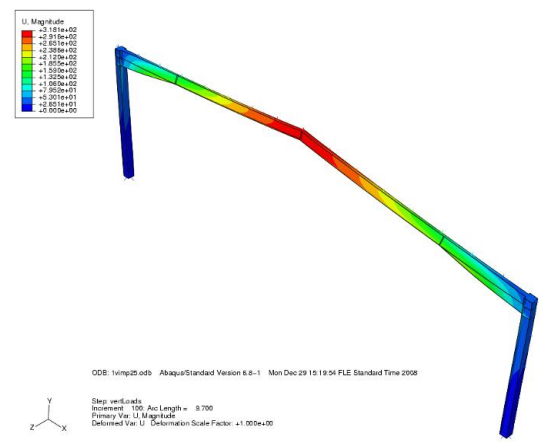 |
| 1.2-4a | 3 | Horizontal | 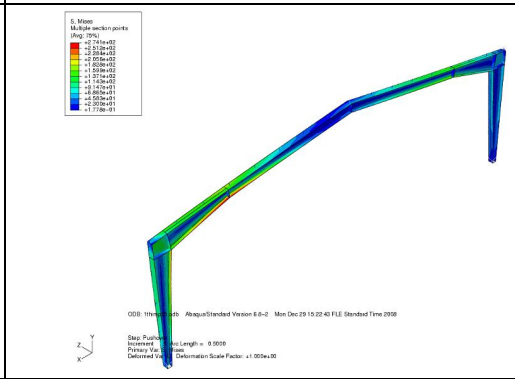 | 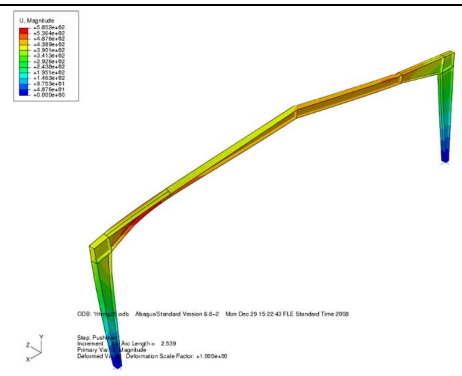 |
| | 4 | Vertical | 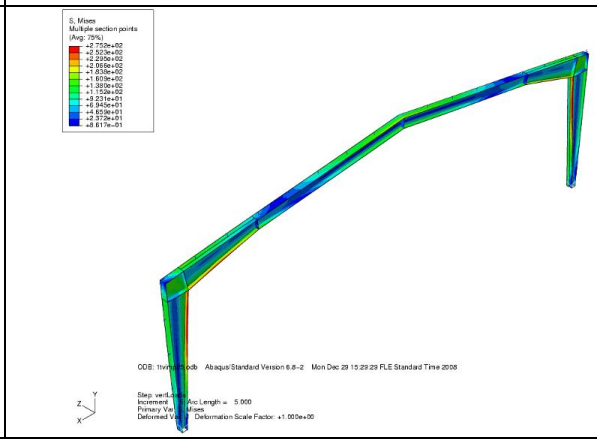 | 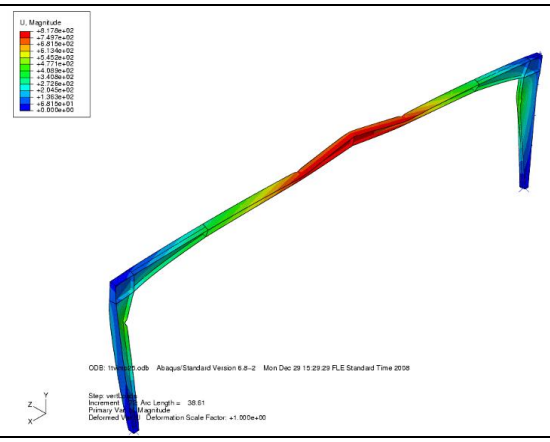 |

| | Nr. | | Yield | Ultimate |
|---|---|---|---|---|
| | | | (a) | (b) |
| 3.6-O | 5 | Horizontal | 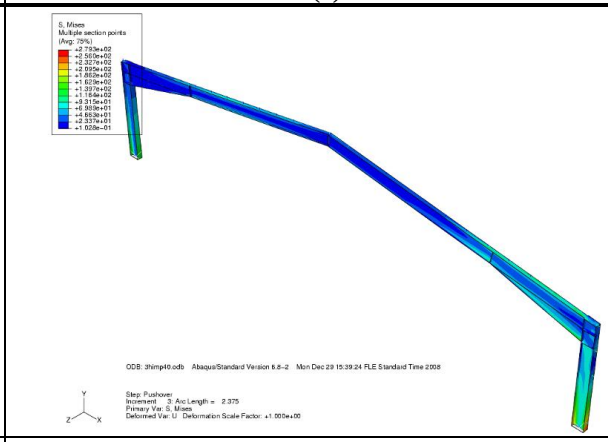 | 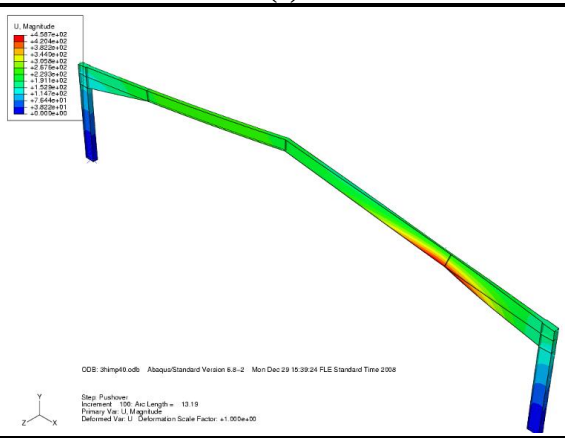 |
| | 6 | Vertical | 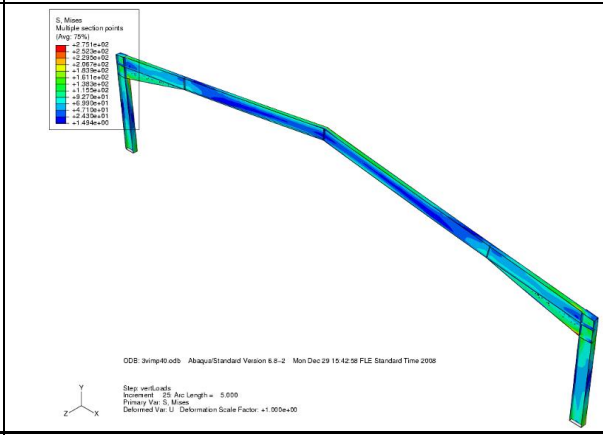 | 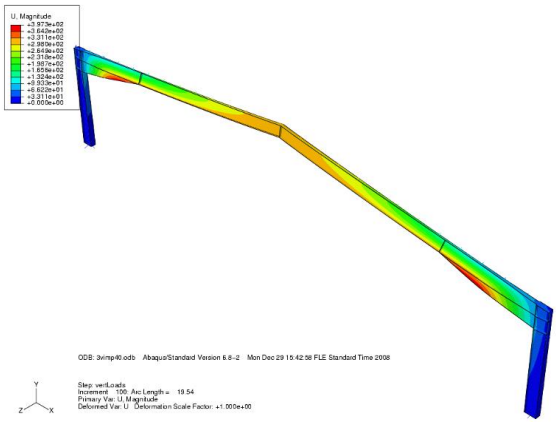 |
| | Nr. | | Yield | Ultimate |
| | | | (a) | (b) |
| 3.6-3a | 7 | Horizontal | 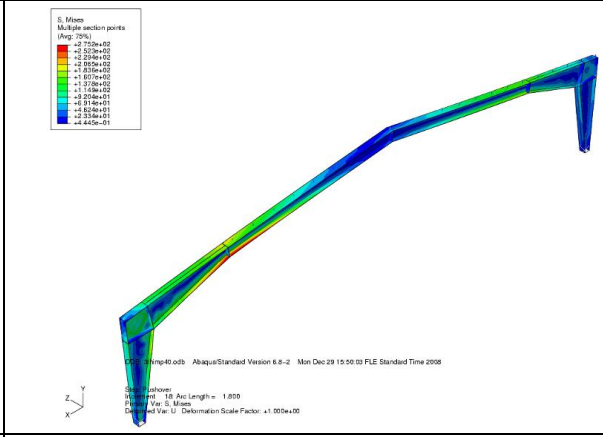 | 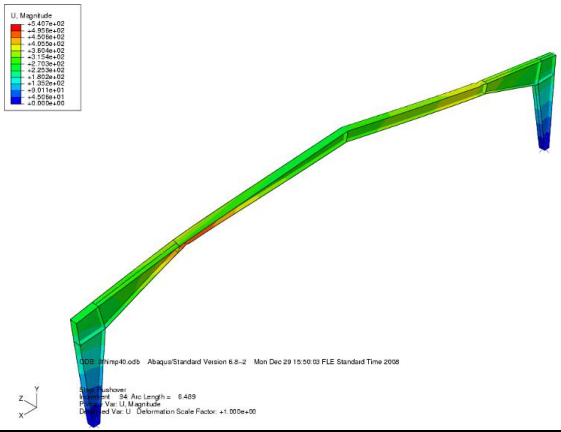 |
| | 8 | Vertical | 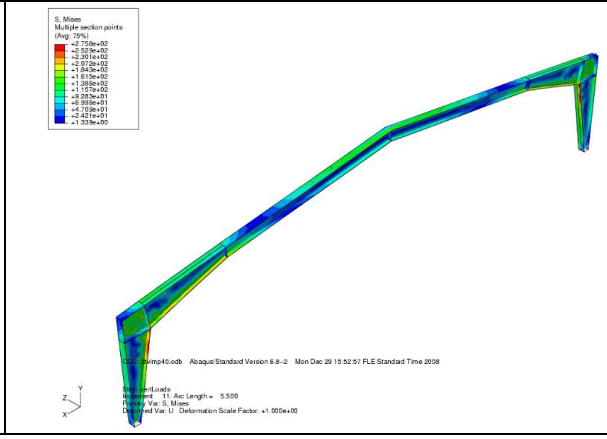 | 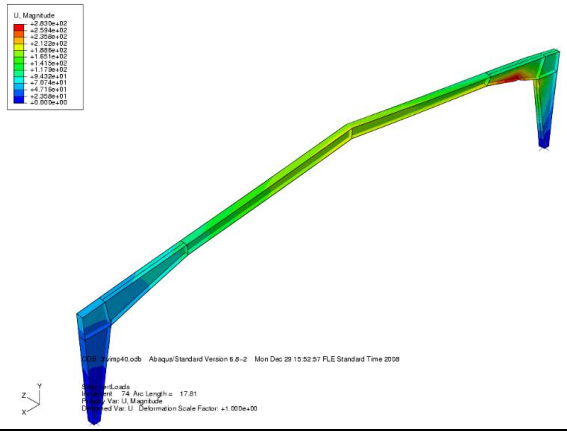 |

| | Nr. | | Yield (a) | Ultimate (b) |
|---|---|---|---|---|
| 2.8-O | 9 | Horizontal | 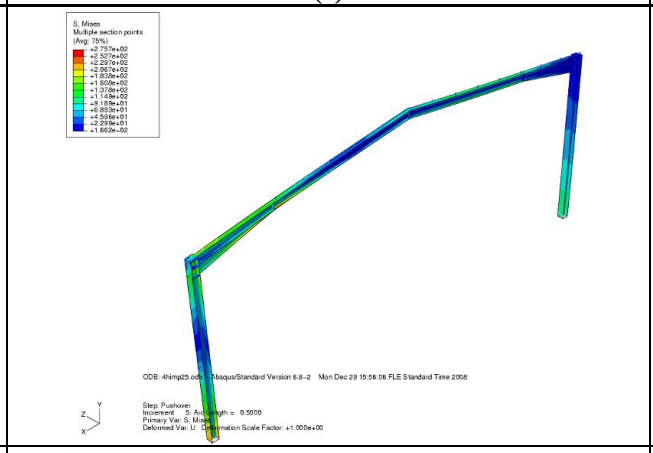 | 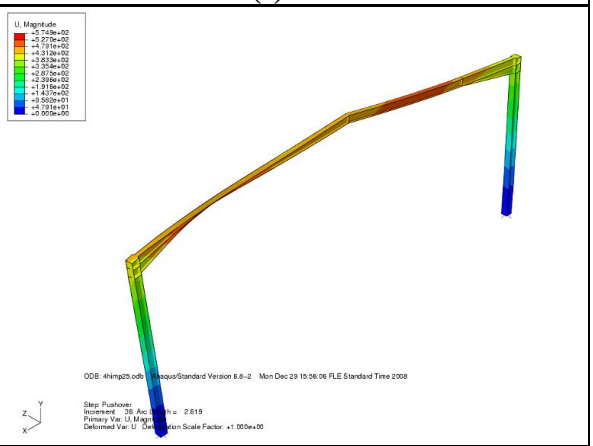 |
| | 10 | Vertical | 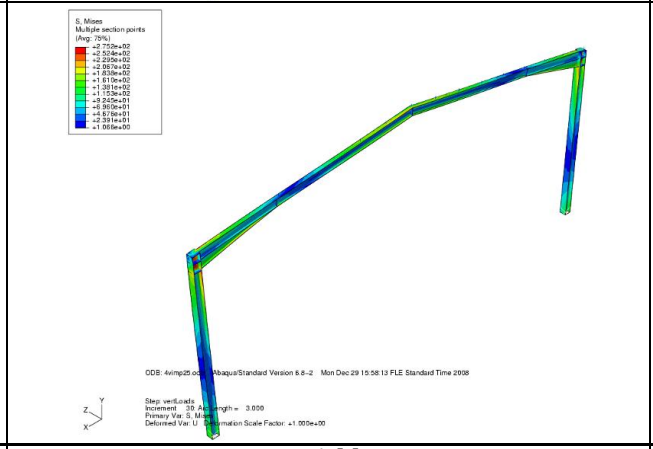 | 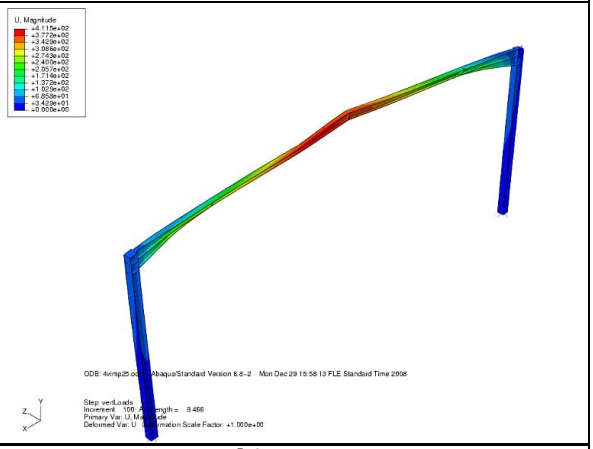 |

| | Nr. | | Yield (a) | Ultimate (b) |
|---|---|---|---|---|
| 2.8-3a | 11 | Horizontal |  | 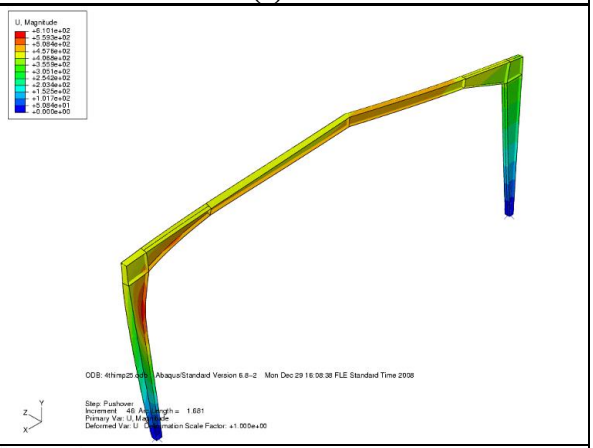 |
| | 12 | Vertical |  | 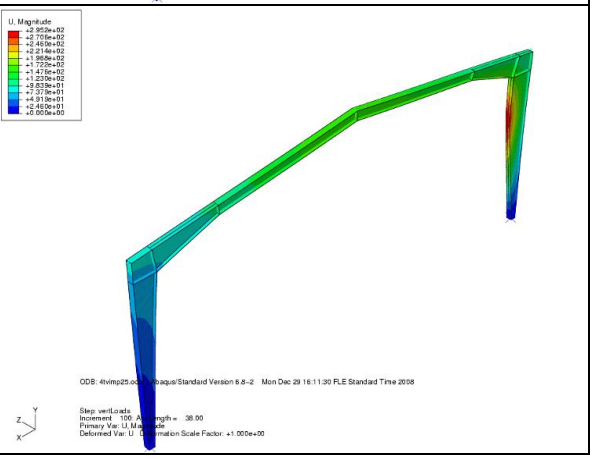 |

| | Nr. | | Yield (a) | Ultimate (b) |
|---|---|---|---|---|
| 3.20-O | 13 | Horizontal | 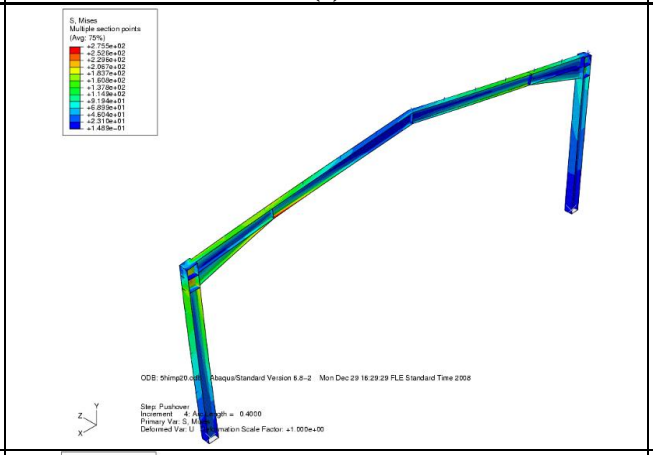 | 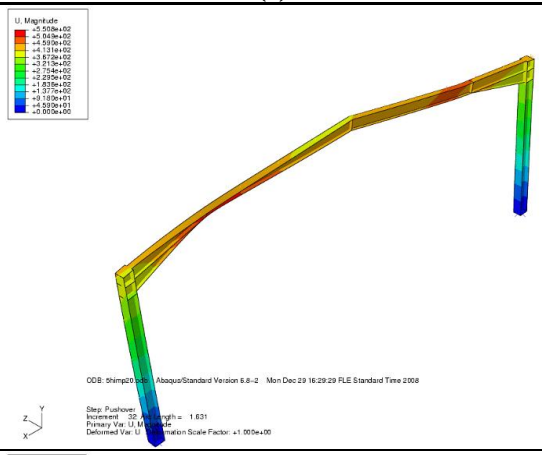 |
| | 14 | Vertical | 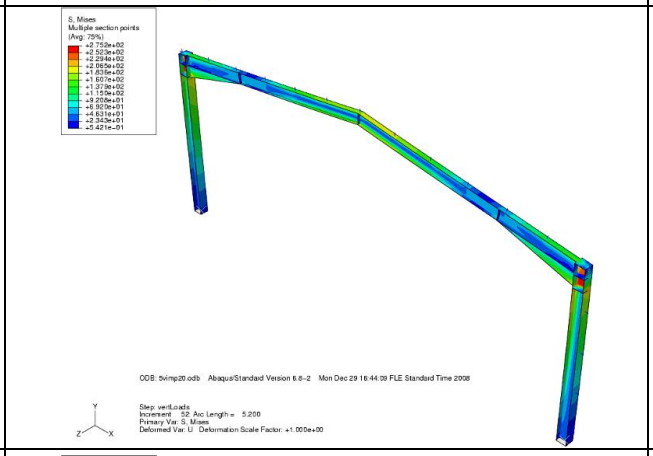 | 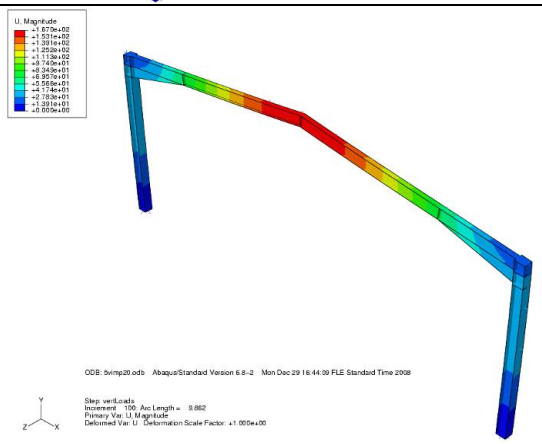 |
| 3.20-2a | 15 | Horizontal | 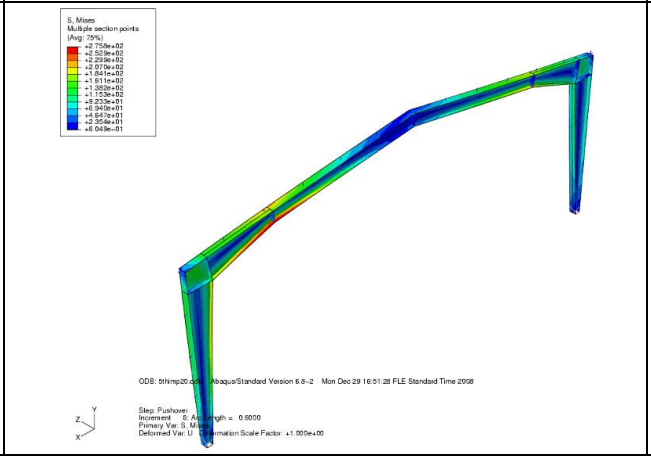 | 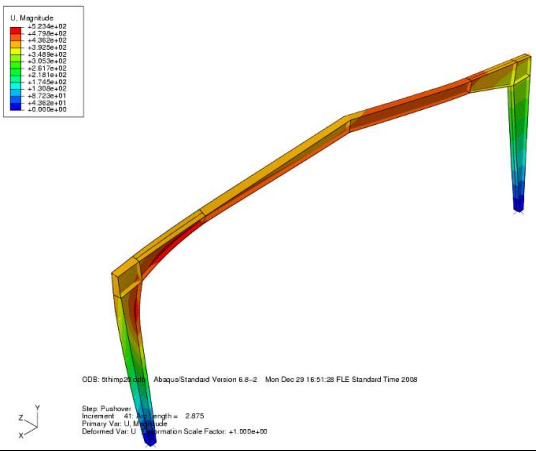 |
| | 16 | Vertical | 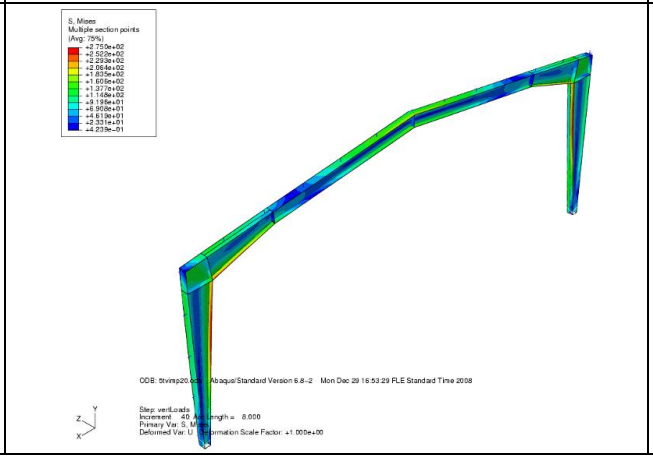 | 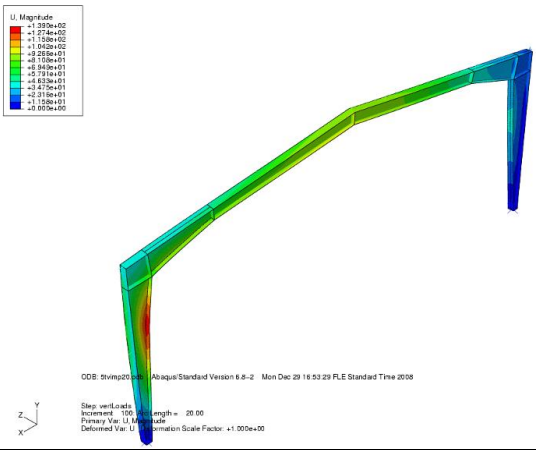 |

*Appendix C. Stress state at yield at the ultimate state (largest displacement converged in ABAQUS).*

| | Nr. | | Yield (Von Mises stress) | Ultimate (Displacement amplitude) |
|---|---|---|---|---|
| | | | (a) | (b) |
| 1.2-450-Fixed | 1 | Horizontal | 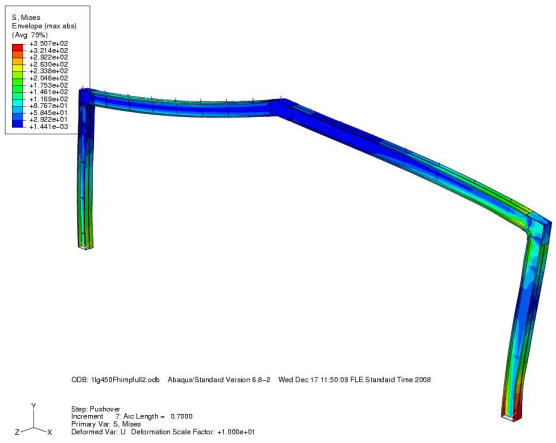 | 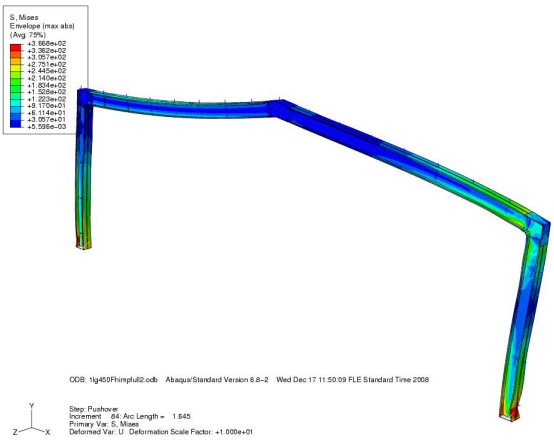 |
| | 2 | Vertical | 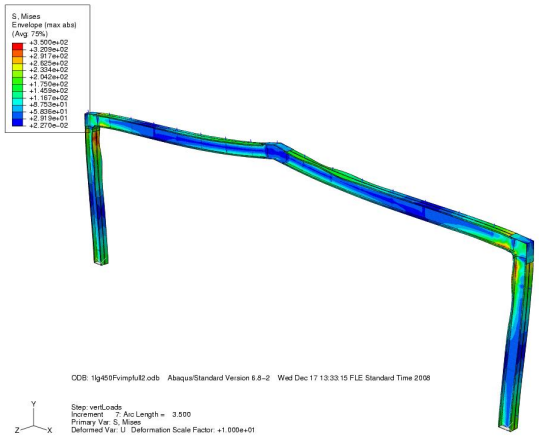 | 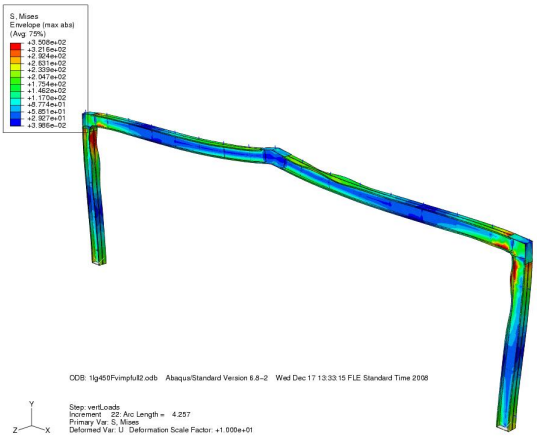 |

| | Nr. | | Yield (Von Mises stress) | Ultimate (Displacement amplitude) |
|---|---|---|---|---|
| | | | (a) | (b) |
| 2.21-500-Fixed | 1 | Horizontal | 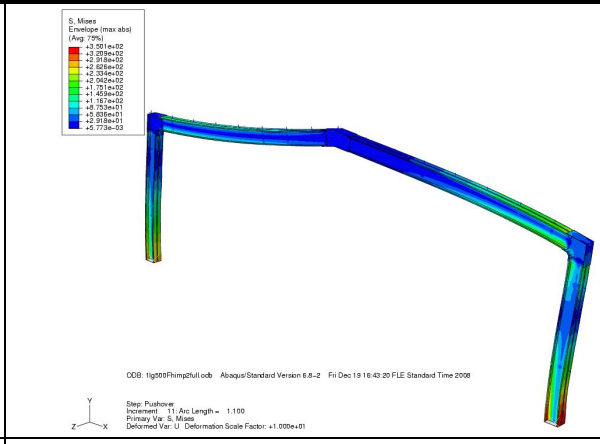 | 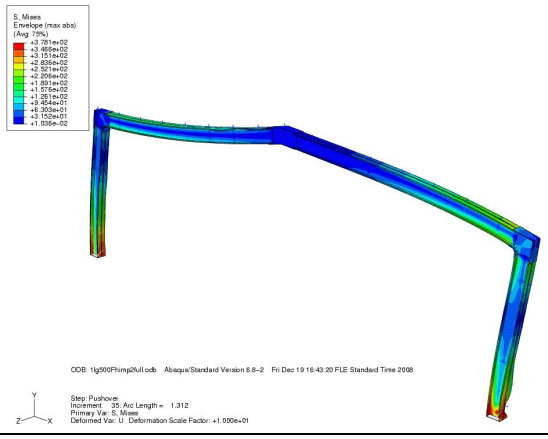 |
| | 2 | Vertical | 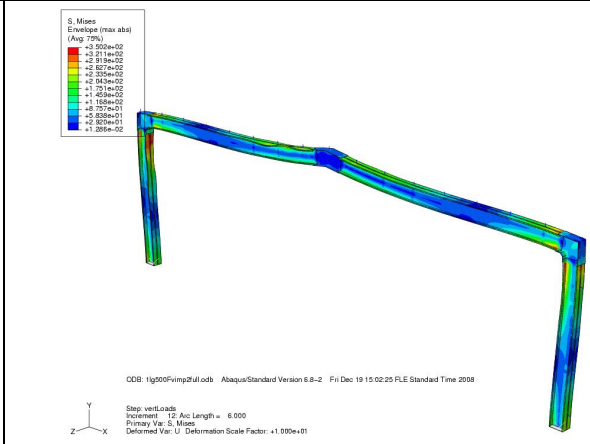 | 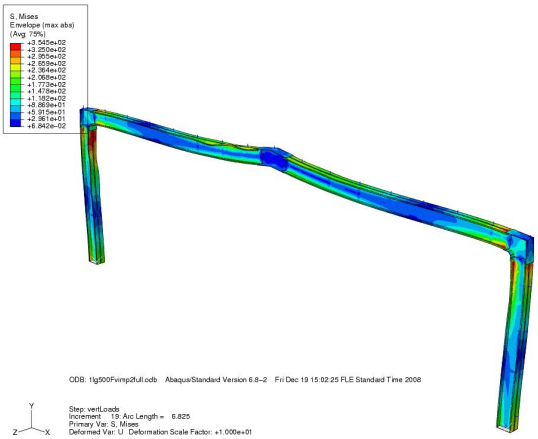 |
| 1.1-400-Pinned | 1 | Horizontal | 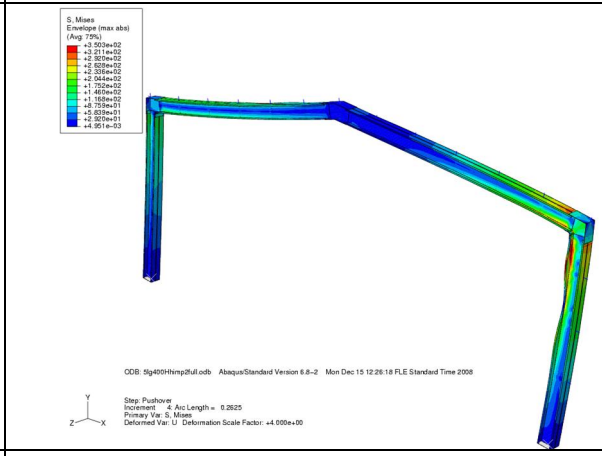 | 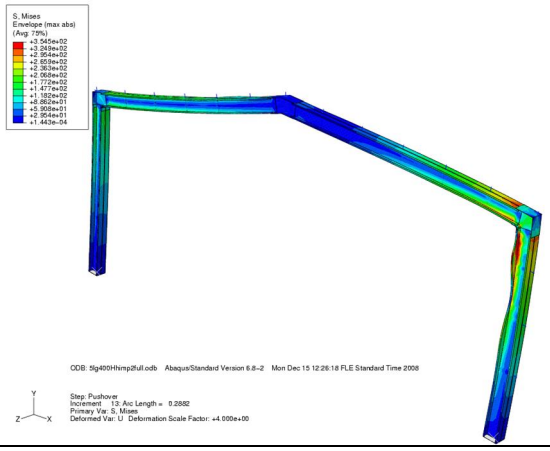 |
| | 2 | Vertical | 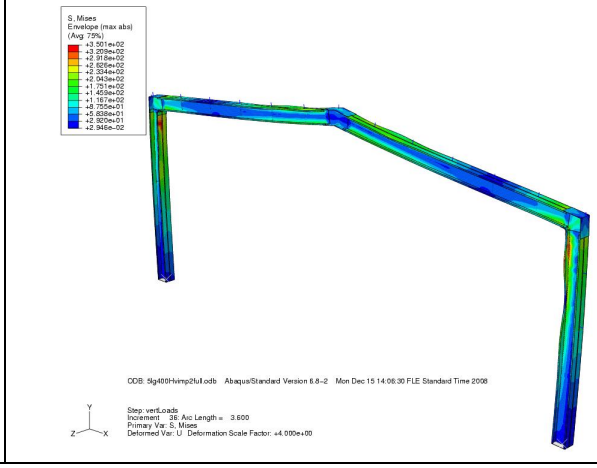 | 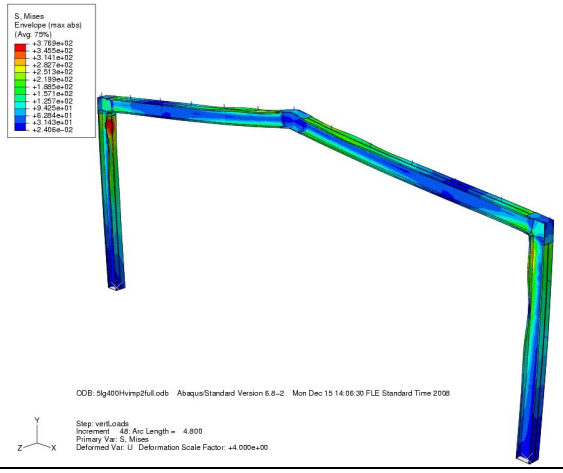 |